Analysis of measurements of Saharan dust by airborne and ground-based remote sensing methods during the Puerto Rico Dust Experiment (PRIDE)

Authors:

J. S. Reid, J. E. Kinney, D. L. Westphal, B. N. Holben, E. J. Welton*, Si-Chee Tsay,
D. P. Eleuterio, J. R. Campbell, S. A. Christopher, P. R. Colarco,
H. H. Jonsson, J. M. Livingston, H. B. Maring, M. L. Meier,
P. Pilewskie, J. M. Prospero, E. A. Reid, L. A. Remer,
P. B. Russell, D. L. Savoie, A. Smirnov, and D. Tanre´

For 26 days in mid-June and July 2000, a research group comprised of U.S. Navy, NASA, and university scientists conducted the Puerto Rico Dust Experiment (PRIDE). In this paper we give a brief overview of mean meteorological conditions during the study. We focus on findings on African dust transported into the Caribbean utilizing Navajo aircraft and AERONET Sun photometer data. During the study midvisible aerosol optical thickness (AOT) in Puerto Rico averaged 0.25, with a maximum >0.5 and with clean marine periods of _0.08. Dust AOTs near the coast of Africa (Cape Verde Islands and Dakar) averaged _0.4, 30% less than previous years. By analyzing dust vertical profiles in addition to supplemental meteorology and MPLNET lidar data we found that dust transport cannot be easily categorized into any particular conceptual model. Toward the end of the study period, the vertical distribution of dust was similar to the commonly assumed Saharan Air Layer (SAL) transport. During the early periods of the study, dust had the highest concentrations in the marine and convective boundary layers with only a weak dust layer in the SAL being present, a state usually associated with wintertime transport patterns. We corroborate the findings of Maring et al. [2003] that in most cases, there was an unexpected lack of vertical stratification of dust particle size. We systematically analyze processes which may impact dust vertical distribution and determine and speculate that dust vertical distribution predominately influenced by flow patterns over Africa and differential advection couple with mixing by easterly waves and regional subsidence.

* Co-Author: Dr. E. J. Welton
             NASA GSFC Code 912
             Ellsworth.J.Welton@nasa.gov

Measurements of Saharan dust by airborne and ground-based remote sensing methods during the Puerto Rico Dust Experiment (PRIDE)

Jeffrey S. Reid[1], James E. Kinney[1], Douglas L. Westphal[2], Brent N. Holben[3], E. Judd Welton[3], Si-Chee Tsay[3], Daniel P. Eleuterio[4], James Campbell[5], Sundar A. Christopher[6], Haflidi H. Jonsson[4], John M. Livingston[7], Hal B. Maring[8], Mike Meier[9], Peter Pilewskie[10], Joseph Prospero[8], Elizabeth A. Reid[11], Lorraine A. Remer[3], Philip B. Russell[10], Dennis L. Savoie[8], Alexander Smirnov[5], and Didier Tanré[12].

[1]Space and Naval Warfare Systems Center-San Diego, San Diego CA.
[2]Naval Research Laboratory, Monterey CA.
[3]NASA Goddard Space Flight Center, Greenbelt MD.
[4]Naval Postgraduate School, Monterey, CA.
[5]University of Maryland, Baltimore County, Baltimore MD.
[6]Dept. of Atmospheric Sciences University of Alabama, Huntsville, AL.
[7]SRI International, Palo Alto, CA.
[8]Rosenstiel School of Marine and Atmospheric Science, University of Miami, Miami FL.
[9]Material Science and Chemical Engineering, University of California, Davis CA.
[10]NASA Ames Research Center, Mountain View CA.
[11]Science and Technology Corp., San Diego CA.
[12]Laboratoire d'Optique Atmospherique, CNRS Universite des Sciences et Technologies de Lille, Villeneuve d'Ascq, France.

Abstract:

For 26 days in mid-June and July 2000, a research group comprised of U.S. Navy, NASA, and university scientists conducted the Puerto Rico Dust Experiment (PRIDE). In this paper we give a brief overview of mean meteorological conditions during the study. We focus on findings on African dust transported into the Caribbean utilizing Navajo aircraft and AERONET Sun photometer data. During the study midvisible aerosol optical thickness (AOT) in Puerto Rico averaged 0.25, with a maximum >0.5 and with clean marine periods of _0.08. Dust AOTs near the coast of Africa (Cape Verde Islands and Dakar) averaged _0.4, 30% less than previous years. By analyzing dust vertical profiles in addition to supplemental meteorology and MPLNET lidar data we found that dust transport cannot be easily categorized into any particular conceptual model. Toward the end of the study period, the vertical distribution of dust was similar to the commonly assumed Saharan Air Layer (SAL) transport. During the early periods of the study, dust had the highest concentrations in the marine and convective boundary layers with only a weak dust layer in the SAL being present, a state usually associated with wintertime transport patterns. We corroborate the findings of Maring et al. [2003] that in most cases, there was an unexpected lack of vertical stratification of dust particle size. We systematically analyze processes which may impact dust vertical distribution and determine and speculate that dust vertical distribution predominately influenced by flow patterns over Africa and differential advection couple with mixing by easterly waves and regional subsidence.

* Corresponding Author, Jeffrey S. Reid, Atmospheric Propagation Branch Code 2858, Space and Naval Warfare System Center San Diego, 53560 Hull St., San Diego, CA 92152, Tel :619-553-1419, Fax 619 553-1417, Email: jreid@spawar.navy.mil

1 **1.0 Introduction**
2   African dust outbreaks into the Mediterranean and north tropical Atlantic Ocean have been
3 recognized and studied for decades [e.g., *Delany et al., 1967; Prospero and Carlson,* 1972; *Ganor and*
4 *Mamane,* 1982]. The Caribbean region, northern South America and the extreme North American
5 southeast have been recognized as important receptor sites for dust transported in the trade winds [e.g.,
6 *Prospero et al.,* 1981; Talbot et al., 1990; *Swap et al.,* 1992; *Swap et al.,* 1996ab; *Westphal et al.,* 1987;
7 *Perry et al.,* 1997; *Formenti et al.,* 2001]. Such transport has been found to be significant in the
8 regions' geochemical cycles, radiative balance and air quality [e.g., *Duce et al.,* 1991; *Swap et al.,*
9 1992; *Tegen and Fung,* 1996; *Prospero,* 1999; *Gao et al.,* 2001]. Further, dust interferes with remote
10 retrievals of such quantities as sea surface temperature measurements [*May et al.,* 1992] and ocean
11 color [*Moulin et al.,* 2001].
12   Saharan dust transport mechanisms into the Caribbean region have been thought to be
13 qualitatively understood for some time [e.g., early analysis by *Carlson and Prospero,* 1972].
14 Subsequent modeling studies and some experimental evidence suggested that the predominant mode
15 involves warm and dry dust-laden air (the Saharan air layer, or SAL) being advected off of the African
16 continent in the easterly trade winds. These easterly trade winds subsequently slide over the westerly
17 near-surface onshore flow of the African monsoon [*e.g., Westphal et al.,* 1987; *Karyampudi and*
18 *Carlson,* 1988]. The theory then suggested that dust is most prevalent in the free troposphere where it
19 is rapidly transported across the Atlantic into the Caribbean region in 5 to 8 days.
20   Despite this qualitative understanding, there is little quantitative data on dust aloft. Sporadic
21 field studies and some lidar work have supported the idea that this is the dominant transport mechanism
22 [e.g., *Prospero and Carlson,* 1972; *Karyampudi et al.,* 1999], but no long term record exists of dust
23 vertical distribution to test this hypothesis. In the last several years, it has been recognized that a low
24 level transport mechanism can occur. *Chiapello et al.* [1995] recognized that during the winter months
25 the near surface on-shore monsoonal flow required to have "classical SAL" transport can weaken,
26 allowing dust to be transported from Africa to sea at lower levels. *Formenti et al.,* [2001] then reported
27 dust in both elevated "SAL" and planetary boundary layers for several days in March 1998 when dust
28 was transported into the Amazon Basin. Even in the middle of the dust season *Karyampudi et al.,* 1999
29 noted that the residual dust can be found in the marine layer underneath the SAL. Recently, in a
30 manuscript describing the vertical distribution of dust found at Puerto Rico during PRIDE, *Reid et al.*
31 [2002] found that dust can be transported to the Caribbean region at lower levels well into the summer.
32 These recent studies have made it clear that dust transport out of Africa is more complicated than may
33 have been first assumed.
34   Variability in dust's vertical distribution causes large uncertainties in many scientific fields
35 including climate, cloud physics, satellite meteorology, geochemical cycles and air quality. In
36 particular, recent sensitivity studies on the affects of dust on the atmosphere's radiative balance have
37 pointed to dust vertical distribution as an important factor for radiative forcing at IR wavelengths [e.g.,
38 *Claquin et al.,* 1998; *Myhre and Stordal,* 2001]. Even if free tropospheric SAL transport were the only
39 mechanism of transport into the Caribbean region, correctly modeling dust transport across the trade
40 inversion into the marine boundary layer would be non-trivial task for transport modeling. But, given
41 the true variability in dust vertical profiles, modeling and parameterizing dust transport is formidable.
42 Clearly a two-dimensional satellite image of regional optical depth is difficult to translate into the three
43 dimensional issues of ocean fertilization, particle concentration at cloud levels for indirect effect
44 studies, and atmospheric visibility.
45   The Puerto Rico Dust Experiment was conducted in July 2000 to better understand these issues
46 of dust transport and radiative forcing in the Caribbean region.   In this manuscript we give an overview

1   of the study objectives, rationale, and resources. The scientific results presented are focused on
2   describing the general transport meteorology of the region. Emphasis is placed on presenting in-situ
3   and ground based remote sensing measurements of dust vertical distribution.
4
5   **2.0 PRIDE Study Rationale**
6   The Puerto Rico Dust Experiment (PRIDE) was conducted by a group of US Navy, NASA and
7   university scientists interested in Saharan dust transport and reducing uncertainty in the dust's radiative
8   effects. The PRIDE campaign had two principal objectives. First, participating scientists wished to
9   better understand the nature of dust transport in order to evaluate/validate the skill the Naval Research
10   Laboratory Aerosol Analysis and Prediction System [*Westphal et al.,* this issue; NAAPS-
11   http://www.nrlmry.navy.mil/aerosol] which predicts the long-range transport and vertical distribution
12   of African dust. This research included issues relating to how models should parameterize dust
13   production, vertical entrainment, advection, and scavenging.
14   The second principal objective of PRIDE was to investigate the extent to which the
15   microphysical, chemical and optical properties of dust particles need to be known before remote
16   sensing systems can accurately determine dust optical depth and estimate radiative flux. This objective
17   is somewhat different from most column closure experiments where some "agreement" is sought
18   between different in-situ and remote sensing systems. It is universally understood that dust is, by
19   nature, both chemically and morphologically complicated and defies easy categorization (e.g., see
20   *Sokolik et al.,* [2001] for an overview). But, it is unclear how and to what extent models and remote
21   sensing systems need to account for this variability.
22   The PRIDE campaign occurred in July, 2000, at Naval Station Roosevelt Roads, Puerto Rico.
23   The July timeframe is considered to be in the first third of the summertime transport season [*Swap et
24   al.,* 1996 b; *Prospero,* 1999]. Roosevelt Roads is located on the far-eastern side of the island of Puerto
25   Rico in mostly unobstructed trade winds (the Isle of Vieques occasionally is upwind when the winds
26   are out of the southeast). This site was chosen in part because in the summer months, Puerto Rico is
27   ideally located as a receptor site for Saharan dust. Both ground based [*Prospero,* 1999] and remote
28   sensing studies [*Swap et al.,* 1996b] place the center of the Saharan dust plume about 2.5 degrees south
29   of the Greater Antilles of the Caribbean region. As will be shown for July 2000, the position of the
30   dust plume from AVHRR pathfinder data was not significantly different from the mean climatology of
31   *Swap et al.,* [1996b].
32
33   **3.0 PRIDE Study Design**
34   The PRIDE intensive operations period occurred for 4 weeks from June 28 through July 24,
35   2001. The PRIDE study field assets included a surface station, two research aircraft, a research vessel,
36   and the Aerosol Robotic Network (AERONET) network of Sun photometers in relevant regions.
37   Satellite sensors employed included the Advanced Very High Resolution Radiometer (AVHRR),
38   Geostationary Operational Environmental Satellite (GOES), Sea-viewing Wide Field-of-view Sensor
39   (SeaWiFS), and the Multi-angle Scanning Radiometer (MISR) and Moderate Resolution Imaging
40   Spectrometer (MODIS) on the Terra satellite.
41   The principal ground site for the mission was located at Cabras Island (Lat. 18.21 N, Long.
42   65.60 W), which hosts a small facility several hundred meters offshore of the main island of Puerto
43   Rico (Figure 1). At the site a University of Miami research trailer was deployed with a weather station,
44   TSI 3-λ nephelometer with backscatter shutter (λ=450, 550, 700 nm), a Radiance Research Particle
45   Soot Absorption Photometer (PSAP) operating at 565 nm, a TSI differential mobility analyzer (DMA)
46   measuring particle sizes between 10 and 700 nm, a TSI Aerodynamic Particle Sizer (APS3300)

1   measuring particle sizes between 1 and 30 μm, and a Micro Orifice Uniform Deposit Impactor
2   (MOUDI) and filter samples analyzed by ion chromatography. A complete description of this package
3   and results can be found in *Savoie et al.* [this issue]. Co-located at the trailer was a Davis Rotating
4   Drum (DRUM) impactor deployed by investigators from the University of California, Davis [*Reid et al*,
5   this issue-b]. Analysis of the DRUM strips yielded elemental concentrations of Na through Cu at four-
6   hour resolution. A NASA Goddard micropulse lidar was also housed inside the trailer (see Section
7   3.3.)
8   A radiation site was also deployed at the Cabras Island facility. Instrumentation included solar
9   and longwave radiometers, diffuse radiometers, a Yankee shadowband radiometer, a microwave
10 radiometer, and a Yankee all-sky camera [*Tsay et al.,* this issue]. Co-located was a hyperspectral
11 radiometer measuring downward flux from 350-3000 nm at ~12 nm resolution [*Pilweskie et al.,* this
12 issue], and an AERONET Sun photometer (see Section 3.2).
13   Two research aircraft and one research vessel operated on the eastern side of Puerto Rico. The
14 first aircraft, the Space and Naval Warfare Systems Center San Diego (SSC San Diego) Navajo, is
15 discussed in full in Section 3.1. The University of Miami also operated a second Cessna 172 during the
16 study [*Maring et al.,* this issue]. The Miami Cessna was equipped with navigation and state
17 instrumentation as well as two Radiance Research nephelometers, a PSAP, and two Met-One optical
18 particle counters. The research vessel, the University of Puerto Rico R/V Chapman, operated off the
19 coast of Puerto Rico from July 3rd through the 7th taking optical depth, ocean leaving radiance, and bio-
20 optical and chlorophyll measurements [*Levy et al.,* this issue].
21   In the following sub-sections detailed descriptions are made of the principal assets utilized in
22 this manuscript: the SSC San Diego Navajo, the AERONET Sun photometer network, and the NASA
23 Goddard micropulse lidar.
24
25 **3.1 Navajo Research Aircraft**
26   The principal aircraft used for PRIDE was a twin-engine, 8 seat Piper Navajo owned and
27 operated by Gibbs Flite Center and contracted by SSC San Diego. During PRIDE, the Navajo flew 21
28 flights (61 hours of data collection over eighty flight hours) near the islands of Puerto Rico, St.
29 Thomas, and St. Croix (Figure 1b).
30   An overview of the Navajo is presented in Figure 2. The Navajo carried a Trimble GPS to
31 provide latitude, longitude, altitude, and vector quantities. A supplemental Trimble TANSVector
32 differential GPS navigational system provided a backup of these quantities as well as pitch ($\pm0.3°$),
33 roll ($\pm0.3°$) and azimuth ($\pm0.5°$).
34   State variable instrumentation included a pressure probe, two temperature probes, and two dew
35 point/relative humidity probes. The static pressure probe was calibrated to ±0.4 mb accuracy. Through
36 the entire study period temperature values from the Navajo Rosemont and Vaisala probes and
37 frequently released radiosondes from the surface were within $\pm0.3°$ C without correction. The
38 EdgeTech dew point hygrometer (±0.5 C), Vaisala relative humidity ($\pm5\%$) probes and radiosondes
39 were within $\pm0.5°$ C of dew point.
40   Radiation instruments onboard included a 6 channel Sun photometer, upwelling and
41 downwelling hyperspectral radiometers, a hyperspectral upwelling radiance instrument, and an Everest
42 infrared thermometer for measuring sea surface temperature. Optical depth measurements were made
43 by the six channel NASA Ames Airborne Sun photometer (AATS-6) for 380, 451, 526, 861 and 1021
44 nm [*Matsumoto et al.,* 1987]. A sixth channel at 840 nm was used to measure column integrated water
45 vapor. Data points were collected every 3 seconds. Vertical profiles of AOT were then used to derive
46 profiles of light extinction under cloud free conditions. This instrument was pre and post mission

1   calibrated by the Langley method at the Moana Loa Observatory, Hawaii.   A manuscript of AATS-6
2   observations during PRIDE can be found in *Livingston et al., [this issue]*.
3   Upwelling and downwelling solar flux were measured with the NASA Ames Solar Spectral
4   Flux Radiometer (SSFR). The SSFR is a moderate resolution flux (irradiance) spectrometer covering
5   the wavelength range from 300 nm to 1700 nm with a spectral resolution of 9 to 12 nm over the spectra
6   range. The dynamic resolution is 15 bits full range, integration time for the each of the spectrometers is
7   nominally 100 ms and spectral sampling rate is approximately 1 Hz. The SSFR is calibrated in absolute
8   power at the Atmospheric Physics Radiation Laboratory and at the NASA Ames Airborne Sensor
9   Facility Laboratory using the same standards used to calibrate various airborne sensors such the
10 MODIS Airborne Simulator (MAS). In the field we calibrated the SSFR before and after flights using a
11 LI-COR field calibration unit which allowed us to monitor the stability of the SSFR over the duration
12 of the experiment. Absolute accuracy of spectral irradiance was dominated by the uncertainty in the
13 NIST primary irradiance standard, nominally 3% across the spectrum. Precision is estimated to be 0.1%
14 over one day and 1% over six months. Detailed findings from the SSFR data can be found in *Pilewskie*
15 *et al., [this issue]*.
16   The spectral reflectance of the ocean's surface in the 350 to 2500 nm range was characterized
17 with a FR-Pro spectrometer from Analytical Spectral Devices Inc. The resolution is 3 nm in the range
18 of 350-1000 nm and 10 nm for longer wavelengths. An 18 degree field of view head was used. This
19 corresponds to a spot size of ~100 m when flying at 300 m above the ground. The instrument was used
20 in reflectance mode in which the radiance is normalized by a baseline value taken of a white barium
21 sulfate plate. The plate measurements are made immediately before boarding the aircraft and
22 immediately upon disembarking. The spectrometer foreoptics were mounted pointing downwards
23 through a hole in the aircraft's body. The angle of mounting varied from day to day, but was fixed
24 during each flight. The pointing angle was chosen to correspond to the view angle of MODIS during
25 overpass on any particular day.
26   Filter samples on polycarbonate substrates were collected through of a small gas inlet on top of
27 the aircraft. It is estimated that the 5 liter per minute flow rate through the inlet was within ±20% of an
28 isokinetic value. Samples were subjected to single particle analysis by a scanning electron microscope
29 (SEM) with Energy Dispersive Analysis with X-rays for elemental qualitative analysis of C, O, and Na
30 through Cu. Results of these analyses can be found in *Reid et al.* [this issue-a]
31   Airborne particle measurements were made with two Particle Measuring Systems (PMS) probes
32 mounted on the Navajo wingtips (the Forward Scattering Spectrometer Probe and the Passive Cavity
33 Aerosol Spectrometer Probe, or FSSP-100X and PCASP-100X, respectively). Both the FSSP and
34 PCASP had undergone the Droplet Measurement Technologies Inc. upgrade to SPP-100 and SPP-200
35 signal processors, respectively.
36   The PCASP measured particle sizes in 20 channels from 0.1 to 3 μm. The instrument was
37 calibrated several times during the mission with polystyrene spheres (n=1.59) and results can be viewed
38 in *Reid et al.* [this issue-b]. Calibrations suggested that a static size binning was acceptable. Particle
39 sizes were adjusted slightly to an assumed particle index of refraction of 1.5, which altered particle
40 binning by <5%. During the mission the PCASP was operated with its deicing heaters on. This along
41 with ram temperature increases the sample temperature by >10°C. Scattering cavity temperature
42 measurements suggest this should have dried particles to <40% relative humidity.
43   The coarse mode aerosol concentration was measured by the FSSP-100 in 20 bins with a
44 nominal size range of 0.75 to 18 μm. Calibrations occurred alongside the PCASP and can also be
45 found in *Reid et al., [this issue-b]*. As discussed by *Collins et al., [2000]*, the FSSP-100 is insensitive to
46 particle size in 1 to ~15 μm range due to inflection points in the Mie size-scattering cross section

curves. To account for this *Collins et al.,* [2000] re-binned the FSSP data into 3 broad bins. However, intercomparisons with other particle sizing instruments performed by *Reid et al.* [this issue-b] suggest that rebinning does not alleviate the problem and that interpreting size histograms from the FSSP (particularly for dust particles) is complex. While Reid et al. discusses the issue at length, a synopsis is presented here.

Because dust is such a heterogeneous mix of various shapes and indices of refraction the response curve is no longer one-to-one. This problem is seriously aggravated by the presence of a Mie inflection point in the response curve for particles in the 4 to 10 μm range (which happens to be where most dust mass is located). While total particle counts and some very coarse sizing can be performed, the higher moment distributions for dust produce unphysical results. For example, the volume distribution for the FSSP yields particle volumes more than an order of magnitude too high. This uncertainty diminishes for the surface area distribution (factor of two too high). The number mode is probably more accurate. Based on regression with University of Miami instrumentation at the Cabras Island site, the FSSP can reasonably estimate dust particle mass (within ±25%). Further, ratioing of the smaller channels with the larger ones can be used to detect variance in the dust size distribution. The ratio of FSSP channel 2+3 with all of the remaining large particles appears to be the most sensitive.

3.2 AERONET Sun Photometer

Two Aerosol Robotic Network (AERONET) Sun photometers were deployed on Puerto Rico for the PRIDE campaign. The principal Sun photometer was at the Cabras Island Site for the duration of the study. The second, installed on July 1, 2001, is still operating at La Pagurara on the South West corner of Puerto Rico (18.0° N, 67.0 ° W). Data from the established Barbados site (13.2 ° N, 59.5 ° W) in the Caribbean and the Capo Verde, (16.75 ° N, 22.9 ° W) and Dakar (14.4 ° N, 17.0 ° W) sites on the west coast of Africa are also used in this analysis [*Smirnov et al.,* 2000b; *Tanré et al.,* 2001]. The AERONET Sun photometers measured spectral aerosol optical thickness (AOT, τ_a) at 6 wavelengths (340, 380, 440, 670, 840 and 1020 nm) plus column integrated water vapor from a 960 nm channel [*Holben et al.,* 2001]. The African and Barbados sites have polarization channels and measure optical depth at only 440, 670, 870, and 1020 nm plus water vapor. Optical depth data was taken every 15 minutes.

3.3 Micropulse Lidar

Measurements of the vertical distribution of aerosols and clouds were made using a micro-pulse lidar system (MPL). The MPL measurements were carried out by the NASA MPLNET project [*Spinhirne et al.,* 1995; *Welton et al.,* 2001a]. The MPL was installed inside the University of Miami aerosol trailer on Cabras Island, Puerto Rico. Continuous measurements were conducted from June 28 to July 24, 2001, except for ± 1 hour of solar noon and occasional power outages.

The MPL is a compact and eye-safe lidar system capable of determining the range of aerosols and clouds by firing a short pulse of laser light (523 nm) and measuring the time-of-flight from pulse transmission to reception of a returned signal. The returned signal is a function of time, converted into range using the speed of light, and is proportional to the amount of light backscattered by Rayleigh scattering, aerosol particles, and clouds. The MPL achieves ANSI eye-safe standards by sending laser pulses at low energy (μJ) and expanding the beam to 20.32 cm in diameter. A fast pulse-repetition-frequency (2500 Hz) is used to achieve a good signal-to-noise, despite the low output energy. The MPL has a small field-of-view (< 100 μrad) and signals received with the instrument do not contain multiple scattering effects.

1   The MPL signals are stored at 1-minute time intervals, with a range resolution of 0.075 km from
2 sea level up to a maximum altitude of 20 km. The raw data were converted into uncalibrated lidar
3 signals, Normalized Relative Backscatter (NRB), using procedures discussed in *Campbell et al.* [2001]
4 and *Welton and Campbell* [2001]. The NRB signals were then analyzed to produce profiles of aerosol
5 extinction and optical depth, and the layer averaged extinction-to-backscatter ratio, using techniques
6 discussed in the Appendix of *Welton et al.* [2001b].
7

8 **4.0 Results**
9 **4.1 Mean Meteorology of the Region**
10   To put the PRIDE results into perspective it is necessary to consider how the meteorological
11 conditions during the study compared to other years. A general description of the mean synoptic
12 conditions for the region can be found in *Giannini et al.* [2000]. The National Center for
13 Environmental Prediction (NCEP) reanalysis fields [*Kalnay et al.*, 1996] for July 2000 were used to
14 compare conditions during the PRIDE observational period to the long term mean (1948-2002).
15 Despite the relatively coarse resolution of these fields, *Fyfe* [1999] has shown that this data set
16 adequately represents the synoptic scale features of the region, including tropical easterly wave
17 structure and propagation.
18   Precipitation estimates based on a blend of outgoing longwave radiation (OLR) anomalies,
19 SSM/I data, and rain gauge data [*Janowiak and Xie,* 1999] indicated there was a significant reduction in
20 precipitation during the spring and early summer season in the northeast Caribbean, extending eastward
21 across the subtropical Atlantic to the western Sahel. In July, negative anomalies were observed of 25 to
22 50 mm below normal in the northeastern Caribbean, which is 30-40 percent below mean values, and
23 75-150 mm deficits in the West Sahel, or 50-100 percent below average. Positive anomalies occurred
24 on the order of 150 mm, 75 percent above normal, in the Gulf of Guinea and northeast coast of South
25 America. Reynolds sea surface temperature (SST) anomalies [*Reynolds and Smith,* 1994], indicated
26 colder than average SSTs on the order of -0.2 to -0.5 °C extending from 5°N to 20°N across the entire
27 Atlantic beneath the main dust track, with opposite warm anomalies of the same magnitude along the
28 equatorial and mid-latitude western Atlantic. In the area of the Atlantic High (20°- 40°N, 30°- 60°W),
29 negative surface pressure anomalies of 2 mb and height anomalies aloft of 10 meters existed below
30 700mb, and conversely, positive anomalies of the same magnitude persisted in the mid and upper
31 levels. Winds from the surface to 600mb were 5-10 m s^{-1} stronger than average with a stronger
32 northerly component. Increased synoptic stability due to reduced surface heat and moisture flux with
33 ridging aloft is proposed as a likely mechanism for the observed positive outgoing long-wave radiation
34 anomalies and reduced rainfall in the subtropical Atlantic discussed above. It is also proposed that the
35 observed anomalous northerly component of the tradewinds resulted in mean movement of tropical
36 easterly waves farther south contributing to observed wetter conditions along the equatorial Atlantic
37 and Brazilian coast, as well as contributing to the abnormally dry conditions in the Caribbean. As can
38 be seen in Figure 3 of the 600mb composite winds and zonal anomaly for July, the observed patterns
39 are consistent with findings by *Grist* [2002] and *Grist et al.* [2002] that the African Easterly Jet (AEJ)
40 (5°- 15°N, 10° W- 20°E) shifts farther southward and is slightly stronger in dry Sahel years. This results
41 in weaker amplitudes for easterly wave disturbances, resulting in weaker wave-associated convective
42 precipitation. As reported in *Karyampudi and Carlson,* 1988, the AEJ or mid-level easterly jet (MLEJ)
43 as the Atlantic extension of this feature is called, occurs on the southern flank of the SAL and is
44 associated with a direct transverse/ vertical circulation and equator-ward ascent due to the enhanced
45 baroclinicity between the warm dry SAL and cool moist equatorial air.

1   Figure 4 depicts observed rainfall for Tambacounda, Senegal and Ouagadougou, Burkina Faso.
2 Despite generally dry conditions in northwest Africa, stations in Burkina Faso and Benin in the ascent
3 region of the MLEJ and near the maximum cyclonic curvature, showed positive precipitation
4 anomalies. *Giannini et al.* [2000] found that cool subtropical Atlantic SST and anomalously dry
5 Caribbean summers are often associated with a cold ENSO phase and a positive SLP anomaly in the
6 North Atlantic High the previous winter. Although the observed ENSO cold phase was consistent in
7 this case, below normal SLP was observed in the North Atlantic High during the 1999-2000 winter,
8 which *Giannini et al.* [2000] correlated with wet (rather than the observed dry) conditions in the
9 northeastern Caribbean the following summer.
10   Because convection associated with the axis of easterly waves usually passed south of Puerto
11 Rico during the study period, weather was fair on most days with the major changes being a wind shift
12 and an intensification and deepening of the easterlies during wave passage. An example of a midday
13 GOES image is presented in Figure 1b. Fair-weather trade cumulus were prevalent through out the
14 day. Morning cumulus usually gave way to clearer skies by noon. Partially obscured skies would occur
15 in mid to late afternoons due to cirrus blow-off from thunderstorms forming on the western side of the
16 island in the lee of the central cordillera. Conditions were predominantly conditionally unstable,
17 typically with convective lines forming in the lee of smaller islands, referred to as "streamers" by local
18 forecasters. Six easterly waves passed through the region during the study period, with wave passage
19 occurring on ~June 28, July 2, 7-8, 12, 14, and 18. Only the waves on July 7 and 12 caused significant
20 precipitation or convective activity in Puerto Rico, and these passed within 6-12 hours.
21   Soundings from San Juan, PR depicting major atmospheric conditions of interest are presented
22 in Figure 5. Figure 5(a), from July 21, 2000 12:00 Z is a typical vertical structure during Saharan Air
23 Layer (SAL) conditions. As reported in *Augestein et al.*, [1974], the classic structure is a well-mixed
24 marine boundary layer (MBL) extending from the surface to about 960mb (500-700 m). Above this is
25 a convective boundary layer (CBL) with fair weather cumulus clouds extending from the MBL
26 inversion to the trade wind inversion at 750-850mb (1,500-2,500 m). The SAL then extends from the
27 trade inversion up to a small capping inversion at 500mb (about 5,000 m). The trade inversion height
28 and strength can vary considerably from day to day, and even show a diurnal cycle on the order of $\pm$250
29 meters [*Augstein et al.*, 1974]. During strong "SAL" conditions the trade inversion was observed to
30 reach a minimum level of ~1 km and be as strong as 3-4 Celsius. *Albrecht* [1979] found that the height
31 and strength of the trade inversion is dictated by the balance between large-scale subsidence and
32 sensible and latent heat fluxes from the ocean surface, and hence the diurnal radiative heating at the
33 surface. Cumulus convection between the MBL and the free troposphere transports heat and moisture
34 upwards from the MBL and thus helps maintain the trade inversion. The trade inversion can evolve in
35 response to disturbed conditions, such as an easterly wave, in as little as 24 hours.
36   Water vapor mixing ratio (ω_v) is often used as an indicator of the tropical atmosphere's
37 structure. Near the surface in the remote ocean environment, the dew point temperature is fairly close
38 to the sea surface temperature. For the Caribbean, the sea surface temperatures and dew points ranged
39 from 22-25 °C, corresponding to ω_v values on the order of 17 to 23 g kg^{-1}. Above the trade inversion in
40 the SAL, the airmass originates overland in Saharan Africa where strong sensible heating results in
41 much lower dew points with ω_v in the 3 to 6 g kg^{-1} range. The well-mixed MBL and the elevated SAL
42 dictate the ω_v profile with relatively constant values in each region and a long gradient in the CBL due
43 to convective mixing. Turbulent processes cause considerable fine structure not shown on this scale.
44 The slope of the vertical ω_v gradient and shape of the ω_v vertical structure in the CBL indicates the
45 degree of mixing occurring between the MBL and SAL through convective processes.

When Puerto Rico was under the influence of an easterly wave, the trade inversion rose in altitude and weakened significantly. This left the middle troposphere very moist. An example is presented in Figure 5(b) with the July 7th sounding from San Juan, Puerto Rico. A cloud layer still forms at the top of MBL (here at ~950 mb). However, many additional cloud layers exist between the MBL and a very weak trade inversion at 700-650 mb. Above this weak inversion was a very dry subtropical high layer. The periodicity through SAL and easterly wave conditions was typically on the order of four to six days with the trade inversion gradually shifting in altitude and strength.

3.2 Optical Depths Over the African Coast and the Caribbean

As part of Figure 1(a) the NOAA AVHRR Pathfinder aerosol optical thickness composite for July 2000 was overlaid. For the PRIDE period, dust dominated the 8° to 27° latitudinal bands across the Atlantic Ocean. Optical depths from the Pathfinder data suggested a July monthly mean value of 0.25 at Puerto Rico, and ~0.4 at the Cape Verde Islands just off of the African Coast (16° N, 24° W). The centerline sloped to the south slightly during transport, being approx. 20° N Latitude at the coast of Africa (passing through the Cape Verde Islands), and staying a roughly constant ~17° N to the Caribbean (~1.3° south of Puerto Rico, AOT ~0.3). This spatial distribution of the African dust was typical for the time period, and was within the 1989-1992 AVHRR climatology found by *Swap et al.,* [1996 b], although, the dust center for the 2000 season was ~4 degrees north of its mean value.

Details on dust loading can be found in the AERONET data from the region. Summary plots of available year 2000 AERONET data for the Cape Verde, Dakar, Barbados, and Puerto Rico (composite of the Roosevelt Roads and La Paguera sites) is presented in Figure 6(a), (b), (c), and (d), respectively. The most continuous record is from Cape Verde, with data available for most of the year. Dakar data was only intermittent with no data available for the winter and spring months. Similarly, the Barbados data was intermittent due to instrument failures. Lastly, the Puerto Rico sites operated without incident from the study start date through the rest of the year.

Despite the intermittent nature of the AERONET data set for these sites, examination of the data is insightful. Most importantly, for the year 2000 fairly typical dust temporal patterns were observed. Large dust events passed over Cape Verde and Dakar in all seasons. These events tended to be episodic in nature in the fall, winter and spring, but with a more sustained level in the summer months. From the Cape Verde data the largest events of 2000 occurred in the late winter and spring. Nine of the highest ten daily averaged optical depths occurred outside the summer season.

At the Caribbean sites, optical depths were low for most of the year with the exception of occasional strong and short dust episodes. At the Barbados site for the May, June, July, August timeframe the commonly observed sustained summer dust feature appears with a maximum in June [*Prospero,* 1999; *Smirnov et al.,* 2000a]. The largest dust event of 2000 to remain coherent during transport into the Caribbean occurred in the last week of May, with large dust-falls being reported over much of the region, and Navy aircraft pilots operating throughout the region reported visibilities aloft <3 km. In Puerto Rico (after June 28), the PRIDE field campaign appeared to have observed AOTs that were also typical for that season, with the dust falling off back to the episodic nature by September 1.

While temporally the dust features appear normal, climatic anomalies discussed in Section 3.1.1 may have manifest themselves in the amount of dust leaving Africa. The 670 nm daily averaged optical depths at Cape Verde for the May, June, July and August timeframes were 0.22±0.12, 0.52±0.22, 0.38±0.19, and 0.42±0.14, respectively (note the July mean value of 0.38 is very close to the AVHRR Pathfinder value of 0.4 discussed above). These monthly averages are lower (but within a standard deviation) than the previous 4 years. *Holben et al.,* [2001] found over the 1996-1999 period daily mean

1 AOTs averaged 0.4±0.3, 0.7±0.3, 0.6±0.2, and 0.4±0.2 over the months of May, June, July and August,
2 respectively.
3   Despite lower dust concentrations at the coast of Africa, dust concentrations in the Caribbean
4 were more normal. Using the Barbados data as an indicator for dust transport into the lower
5 Caribbean, the AERONET 670 nm mean AOTs were 0.16±0.12, 0.34±0.10, and 0.26±0.13, for the
6 May, June and July 2000 timeframe, respectively (recall the Barbados site became more intermittent
7 after July). These values are very near the 870 nm mean values given by *Smirnov et al.* [2000b] of
8 0.18±0.10, 0.34±0.22, and 0.24±0.14, for May, June and July, respectively, 1996 to 1999 timeframe.
9 Correcting for wavelength differences increase the Smirnov et al. values by no more than 0.03.
10   Details of dust optical depths in Africa and the Caribbean during the PRIDE period can be
11 found in Figure 7(a) (b), (c), and (d) where daily average AOTs for the June 20-July 25 period are
12 displayed for Cape Verde, Dakar, Barbados, and Roosevelt Roads, respectively. The Roosevelt Roads
13 data plot includes data from the La Paguera site for July 3, 4, 22, and 23 when no cloud screened data
14 was available.
15   During the PRIDE field campaign, Puerto Rico experienced 6 significant dust episodes, with
16 peaks in AOT on June 28/29, and July 5, 9, 15, 21, and 23, 2000. Dust storms in Africa recurred
17 roughly every 4 to 6 days. Navy Aerosol Analysis and Prediction System model runs suggest these
18 events left the coast of Africa on June 23/24 and 29, and July 4, 10, and 15/16. [*Westphal et al.*, this
19 issue]. *Westphal et al.* [this issue] corroborated these times by available SeaWiFS data. The difference
20 in the Puerto Rico and Cape Verde peak AOTs suggest a ~6 day transit time across the subtropical
21 Atlantic Ocean. During the PRIDE field campaign, the average daily 670 nm optical depth at
22 Roosevelt Roads was 0.25±0.12. For the five peak dust days events at Puerto Rico, AOTs were
23 0.46±0.11. Barbados had similar values with a mean 670 nm AOT value of 0.26±0.12 and an average
24 AOT of 0.40±0.06 for the 5 highest days. Four of the 5 events observed at Puerto Rico were also seen
25 at Barbados. Arrival times varied at Barbados but were usually within a day. High levels of dust were
26 also found at Barbados on July 13 and 23 that were not seen at Puerto Rico.
27   As is expected for coarse mode particles the wavelength dependence of the dust was spectrally
28 flat. Figure 8(a) shows spectral AOT plots for 3 dust events plus a background day (AOT ~0.12) at
29 Cape Verde. The 440-870 Angstrom exponent was fairly static with study averages at 0.24±0.06. Such
30 a low value suggests that at no time was the region was not significantly influenced by fine mode
31 particles such as pollution from Europe or Smoke from Africa.
32   Shown in Figure 8(b) are the daily average spectral AOT data for four dust events and clean
33 marine day at Roosevelt Roads. Mid-visible Angstrom exponents (440-870 nm) at this site were also
34 low with study averages at 0.19±0.11. On the 7 cleanest days with AOT<0.1, the 440-870 nm
35 Angstrom exponent increased only to 0.40+0.13. Similar to the Cape Verde case, these values
36 demonstrate that coarse mode particles (whether sea salt or dust) dominate the atmosphere's optical
37 depth at Puerto Rico.
38
39 **3.3 Navajo Flight Operations**
40   Over the PRIDE field study, the Navajo performed twenty-one research flights for eighty flight
41 hours. Data collection occurred for 61 of these hours. A summary of Navajo flight data collection
42 times and atmospheric conditions is presented in Table 1. Flights occurred at least every other day, and
43 typically began at 9:00-10:00 local Atlantic Time (13:00-14:00 UTC) in order to have the aircraft in
44 position for the Terra overpass time of ~11:00 AM local time. The Navajo flew on 4 of the 5 heaviest
45 dust days at Puerto Rico (the exception being July 9th).

1 	Each flight began with a continuous vertical profile from 30 m to ~5,000 m over the Cabras
2 	Island aerosol/radiation site to characterize the local environment. If the site was totally cloud
3 	covered, we would move no more than 15 km to the southeast. Once at altitude the Navajo proceeded
4 	to a cloud-free region 50 to 100 km away. In all but three cases this was in the region roughly bounded
5 	by Cabras Island, St. Croix (17° N, 65° W) and St. Thomas (19° N, 65° W). On July 8, this region
6 	was heavily cloud covered and the aircraft flew offshore the west end of Puerto Rico. On July 22 and
7 	24, the aircraft proceeded south from Cabras Island 100 and 200 km, respectively, to sample heavier
8 	dust concentrations.
9 	Once at this secondary location the Navajo performed a descending profile to the surface. On
10 	selected flights intermittent level legs of ~10-20 km in length were included in the descent for making
11 	radiometer measurements. Once at the surface, the Navajo proceeded for 50 to 100 km in a generally
12 	north-south direction at 30 to 100 meter altitudes to make optical depth measurements with the AATS-6
13 	to validate Terra satellite products. The Navajo then either performed a final vertical profile to the top
14 	of the dust layer or returned directly back to Roosevelt Roads. By the end of PRIDE, the Navajo had
15 	performed 58 vertical profiles on 21 days.
16 	During the PRIDE study period, the Navajo took measurements in a variety of conditions, from
17 	days with very strong trade inversions and fair weather, to very moist atmospheres under the influence
18 	of easterly waves. As discussed in the PRIDE preliminary findings paper by *Reid et al.* [2002], we also
19 	found dust not only in the SAL layer, but in a wide variety of vertical distributions. In the following
20 	sections, we divide our measurements into three groups. First we discuss days with very clean (little
21 	dust) background conditions. Second, we present data from observed dust events which conform to the
22 	SAL dust transport conceptual model. Lastly, we examine days that have variable dust vertical
23 	distribution and do not fit into any established classification.
24
25 	*3.3.1 Clean Marine Conditions*
26 	On the July 8, 11, 17, and 19 flights AOTs in the vicinity of Puerto Rico were below 0.08.
27 	These observed optical depths are consistent with clean marine environments [*Smirnov et al.*, 2002]. As
28 	with other times during the study, Angstrom exponents were low during clean periods at 0.47, 0.25,
29 	0.34, 0.25 for the 8, 11, 17, and 19 dates, respectively, indicating that coarse mode salt particles
30 	dominate the atmospheric optical depth. At the surface, easterly trade winds were consistent in the 5-7
31 	m s^{-1} range. Skies were mostly clear over the ocean for the July 11, 17 and 19 episodes, with <15%
32 	coverage by fair trade cumulus and occasional cumulus congestus. For July 8, the region was under the
33 	influence of an easterly wave to the south, with a much more moist lower troposphere and 20%
34 	coverage of cumulus congestous, and >60% thick cirrus coverage. Savoie et al. [this issue] found dry
35 	sea salt concentrations to be ~15-20 µg m^{-3} on these days, compared with dust concentrations <5 µg m^{-3}
36 	during the flight.
37 	Summary profiles of atmospheric conditions in Cabras Island region can be found in Figure 9.
38 	In the first column, soundings of temperature (T), dew point (T$_d$), equivalent potential temperature (θ$_e$),
39 	and water vapor mixing ratio (w$_v$) are presented. In the second, summary soundings of coarse mode
40 	particle concentrations and estimated coarse mode mass from the FSSP is presented. Number
41 	concentrations are split between the 1.5-3 µm and 3-17 µm ranges. To estimate mass concentration the
42 	surface area-to-mass regression used in *Reid et al.* [this issue-b] is utilized. In the third column,
43 	sounding plots from the PCASP are presented. Here the data is broken into two categories. First, the
44 	estimated mass of particles (assuming a density of 1.4 g cm^{-3}) less than 0.3 µm in diameter is given.
45 	These particles are not likely to be from aolean sources, but rather pollutants from Africa or secondary
46 	particles produced over the ocean. Also shown is the estimated mass concentration of particles in the

1   0.3 to 1.1 μm range, that are more likely to represent small dust particles and some sea salt (for dust we
2   assumed an effective density of 2 g cm^{-3}).
3   All of the background days studied had similar characteristics. The MBL from the surface to
4   500-700 m was clearly evident from the constant values of θ_e and static values of ω_v at ~18 g kg^{-1}.
5   Above the MBL was a thick, moist and neutral CBL that extended through several weak inversions up
6   to ~2000 to 3000 m. In the CBL, water vapor mixing ratio tended to monotonically decreased to a
7   value of 10 g kg^{-1}. These conditions suggest that moist convective mixing was responsible for air
8   exchange between MBL and aloft. Above the weak trade inversions were occasional ~1000 m deep
9   layers topped by a strong subsidence inversion at ~3000-4000 m. The layer defined by these last two
10   inversions tended to have a ω_v of 2-10 g kg^{-1} and could have had continental origins or have been a
11   remnant of a previous subsidence inversion. This may be considered a "SAL", but its definition is
12   rather weak. Above the subtropical subsidence inversion, the air dried rapidly with w_v dropping to less
13   than 1 g kg^{-1}.
14   The fine and coarse mode particle vertical distributions were defined by the inversions. Both
15   fine and coarse particle mass concentrations were at a maximum at the surface and MBL. Coarse mode
16   sea-salt particles dominated the MBL with ambient concentrations increasing to a maximum at cloud
17   base due to hygroscopic growth. Occasional brushes with clouds caused peaks in the FSSP number
18   concentrations and mass at the MBL top. Since the PCASP is dried, it shows a falloff with altitude.
19   There is large discrepancy in magnitude between the regression mass and 1.5-3 μm mass estimation in
20   the FSSP, indicating the coarse mode is indeed dominated by large sea-salt particles. Between the week
21   inversions of CBL some thin layers of both fine and coarse mode particles are observable. However,
22   coarse mode particles fell to below detectable limits at 2000 m.
23
24   *3.3.2 Strong SAL Conditions*
25   Only over the last five days of the PRIDE study (July 20-24) did we observe dust vertical
26   distributions that were considered "typical" for Saharan dust transport into the Caribbean. Vertical
27   sounding plots for July 20, 21, 22, and 23 flights are presented in Figure 10. The case on the 24th was
28   very similar to the 22nd. As with most of the clean marine days, local weather during the periods was
29   fair, with scattered trade cumulus over the oceans and afternoon thunder storms developing on the west
30   side of Puerto Rico.
31   As discussed in Section 3.3.1, July 19th could be considered a clean marine background day
32   with minimal dust detected. On the late evening of the 19th, the first signs of the dust event appeared at
33   Puerto Rico. By the morning Navajo flight of July 20th, the profile mid-visible AOT increased from
34   0.06 to 0.27. A moist MBL and CBL was topped by a moderate trade inversion base at ~2800 m. A
35   SAL is evident from the sounding with a w_v values being a static 3-5 g kg^{-1} in the 3000-5800 m range.
36   Such a value is clearly from continental origins. If w_v were lower, it would be too dry to be from
37   Africa, and higher it would have indicated marine influence. The SAL is topped by a subtropical
38   subsidence inversion at 5800 m. Particle soundings show a clear dominance of dust particles in the
39   SAL between 2300 and 4500 meters (note that the top of the dust layer is lower than the top of the
40   SAL). Distinct layering is also visible at the 3500 and 4200 m marks. An additional thin particle layer
41   is also visible in the 4800-5600 m region.
42   Atmospheric dust is best seen in the FSSP 1.5-3 μm and PCASP 0.3-1.1 μm data. These
43   particles are too small to be sea salt, and too large for accumulation mode anthropogenics. Comparison
44   of FSSP number concentration in the 1.5-3 and 3-17 μm ranges suggests that there are only slight shifts
45   in particle size with altitude. A crossover does occur above 4400 meters, at the top of the dust layer.
46   As counting statistics suggest that sufficient large dust particles were counted in the FSSP, this change

1   in size is likely due to depletion of the larger dust particles to gravitational settling. PCASP soundings
2   in the 0.3-1.1 µm range followed the FSSP soundings very well, mirroring the layered structure,
3   although some height differences exist due to fallout. Since, these particles do not have appreciable fall
4   velocities (~3 m per day for 1 µm particle), this PCASP data probably is the best tracer that describes
5   the vertical distribution of dust without the influence of fallout. Comparisons of the particle mass in the
6   PCASP and FSSP size ranges indicates a dominance of coarse mode particles (25:1 mass ratio) which
7   is consistent with the low Angstrom exponents found at the AERONET Sun photometer site. While
8   accumulation mode particles <0.3 µm do show a slight increase in the SAL it does not strongly mirror
9   the layering structure of the dust. This increase might be dust in combination with low concentrations
10 of anthropogenic primary or secondary particles also being transported across the Atlantic Ocean with
11 the SAL airmass. Regardless, large dust particles clearly dominate the atmospheres AOT.
12   By the July 21 flight, dust optical depths reached a mid-visible profile AOT of 0.35.
13 AERONET and lidar (discussed later) suggests this was in a slight dip in the dust AOT of 0.5
14 approximately 4 hours before and after the flight. For the flight period dust concentrations were
15 slightly lower than the July 20th, but the SAL was considerably deeper. By the 21st the SAL had
16 dropped ~1000 m to 1350 m and strengthened to 3 C. However, the well defined trade inversion did
17 not delineate the start of the dust layer in the SAL. A 500 m thick region with slightly suppressed w_v
18 values was relatively particle free. At 2000 meters, a slight increase in dew point and w_v to 5 g kg^{-1}
19 coincide with the increase in particle concentration within the SAL. Dust layering was also present on
20 this day. Most shifts in particle concentration were accompanied with small shifts in w_v.
21   Qualitatively, it also appears as if there is a shift in particle size distribution over the previous
22 24 hours. In Figure 10 (a)-2, we find that the ratio of 3-17 µm to 1.5-3 µm particles on July 20th in the
23 SAL is approximately 3:2. For July 21st (and all subsequent days), this ratio reverses, to approximately
24 2:3. As on July 20 clear upper level dominance of dust is best seen in the FSSP 1.1-3 µm and PCASP
25 0.3-1.1 µm ranges. The accumulation mode particles in the PCASP(<0.3 µm bin) also somewhat tracks
26 the coarse mode in that a clear layer is in the SAL, but clearly the vertical structure within the SAL is
27 more concentrated at lower levels, and almost no layering is present. This also suggests the presence of
28 anthropogenics being transported across the Atlantic Ocean with the dust. In the MBL and CBL, the
29 FSSP regression mass values suggests some particle enhancement below the main dust layer. Filter
30 measurements by *Savoie et al.* [this issue] suggest roughly half of this increase is due to sea-salt.
31   By July 22 AOTs dropped significantly to 0.11 but the dust was still dominant in the SAL.
32 Over the previous 24 hours, the trade inversion weakened slightly and increased in altitude to 2000
33 meters. The supra-SAL subsidence inversion also descended, leaving the dust in a layer only 2000 m
34 thick. Further, fine mode particle concentrations were near the clean marine background conditions.
35 Finally, on July 23, the Navajo caught a final pulse of this event, and AOTs increased back up to 0.3.
36 Here, the subsidence inversion remained at 4000 meters, but the trade inversion descended to 1650 m.
37 Of all of the days monitored, this day appeared to have the most stratification in dust. However, like
38 the previous day, accumulation mode particles were extremely low in number and had almost no
39 correlation with the dust.
40
41 *3.3.3 Lower Level Dust Transport*
42   The dust event discussed in Section 3.3.2 fit well with the *Karyampudi et al.,* [1999] description
43 of summertime SAL dust outbreaks from Africa and corroborate the observations in the region by
44 *Prospero and Carlson* [1972]. Dust was dominant above the trade inversion in relatively dry (w_v ~5 g
45 kg^{-1}), neutral-stable air. Dust was also fairly well distributed in the SAL, with some layering present.
46 The SAL was topped by a subtropical subsidence inversion, above which virtually no dust existed.

1   Based on these findings, it would seem to be a logical conclusion to estimate dust particle distribution
2   based on atmospheric sounding profiles and an independent optical depth by confining most of the dust
3   between the trade and subsidence inversion. However, in the first half of the PRIDE study, dust
4   vertical distribution was considerably more variable.
5   Figure 11 shows Navajo vertical profile data over the Cabras Island for four days at the
6   beginning of the study. The very first day of the mission, June 28, had the highest optical depth of dust
7   during a Navajo flight . Skies were ~50% cirrus covered, but profile AOTs in clear patches were on the
8   order of 0.5. Subtracting the mean from clean marine days, this implies dust AOTs were on the order
9   of 0.41. At times reported visibility by aircraft in the region dropped below 6 km during the day. The
10   island of Vieques ~10 km away from the Cabras Island site, was only barely visible at times. While
11   filter sampling had not started during the study yet, based on Navajo FSSP and PCASP data we
12   estimate that dust concentrations at the surface were at least 100 μg m^{-3} during the flight. From
13   visibility reports on this day, at times the dust concentration must have been several times higher.
14   The dust vertical distribution and atmospheric sounding for this flight was unlike any other
15   during the study. Like the July 21 SAL case, the trade inversion was strong and relatively low at 1100
16   m. The upper level subsidence was lower than the July 21 case by ~1000 meter, confining the dust to
17   altitudes below 4000 m. What was remarkable about the sounding however, was that the atmosphere
18   was relatively dry below the trade inversion. In all other flights during PRIDE, w_v values were ~18 g
19   kg^{-1} throughout the MBL, typical for the tropics. For the June 28 case w_v was 18 g kg^{-1} at the surface,
20   but decreased rapidly to ~12 g kg^{-1} by 500 m indicating that the atmosphere was not well mixed at the
21   surface. Further, cloud base was not at ~500 meters as it was in previous days, but rather at the trade
22   inversion itself. Above the trade inversion a SAL was clearly evident with w_v constant at the expected
23   value of 5 g kg^{-1}.
24   Both the FSSP and PCASP soundings indicate that, contrary to what is assumed, dust reached
25   maximum concentrations below the trade inversion. In the SAL, the FSSP suggested dust
26   concentration on the order 50 μg m^{-3}, slightly higher than the SAL case days shown in Section 3.3.2.
27   Below the trade inversion, values reached 100 μg m^{-3}. As was typical at cloud base, particle volumes
28   of large particles increased due to deliquescence and occasional cloud droplets (note the increase was
29   not as substantial in the 1.1-3 mm bin and the PCASP data).
30   On the following days of this large event, dust vertical distributions varied considerably. On the
31   July 3rd flight which exhibited a week trade inversion at 2000 m, dust was strictly confined to below the
32   trade inversion, despite the presence of a clear SAL layer between 2000 and 4000 meters. For the
33   flight on July 4th (which was similar to the June 30th flight not shown), dust was more evenly
34   distributed with slight maximums at the very top of the SAL and at the surface. By July 5th (which is
35   similar to the July 6th flight not shown) a reasonably 2 C trade inversion had developed at 2000m , but
36   dust concentrations appeared to be constant across the inversion. This is similar to the vertical
37   distributions shown by *Prospero and Carlson* [1972] for the May-June time period during the BOMEX
38   study, but with considerably higher concentration.
39   Clearly, there was a shift between dust vertical distribution between the beginning and end of
40   the PRIDE study. This shift occurred without significant changes in the atmospheric thermodynamic
41   sounding (with the exception of June 28th). The shift from "mixed" or "low level" transport to the more
42   classic "SAL" transport did not happen suddenly, but rather over a period of 10 days. Figure 12
43   presents four flight soundings during this transition period. Like previous profiles, on July 10 a SAL
44   was present, although the subsidence inversion was lower at 3500 m. Trade cumulus clouds were
45   scarce, with the only clouds being from streamers coming off of local islands. Also, like the event on
46   July 5, dust appears to be fairly well mixed, with the regular exception of particle growth at the top of

the MBL where relative humidity was at a maximum. Using the 1.5-3 μm and PCASP 0.3-1.1 μm channels as an indicator of dust, the vertical distribution is somewhat bi-modal, with dust maximums in the SAL and in the MBL and a clean layer in between. By July 13, the bimodal nature becomes more evident. For the July 15 dust maximum at Cabras Island (AOT =0.26), the dust appears to have shifted into the SAL transport pattern with mostly aloft above a strong trade inversion at 1100 m. As the atmospheric dust loading began to tail off by July 16 (AOT=0.42), a clear SAL dust layer was evident from 2000 to 4000 km, a separate lower level dust layer was found in the MBL with concentrations rivaling those aloft. In fact, despite the decrease in dust AOT between the two days (daily average AERONET AOTs of 0.48 to 0.24 for the 15th and 16th, respectively) the 24-hour filter samples taken by *Savoie et al.* [this issue] show a mean increase in surface dust concentration from ~30 to ~50 μg m^{-3}.

3.3.4 Dust Regional Variability

During the PRIDE study we did not detect much variability in the dust vertical distribution in the Puerto Rico region on the multiple vertical profiles of each Navajo flight. This is probably in part due to the limited range of the aircraft on most days. However, there were several occasions when the gradient of dust was so strong that it was easily detectable. The four strongest cases are presented in Figure 13, where we present the atmospheric temperature and dew point sounding, FSSP particle concentration in the 1.5-3 μm range, and the aircraft flight track overlaid on the GOES –8 visible image from the beginning of the flight.

Variability in dust properties took several forms. In the simplest cases dust concentrations simply shifted uniformly in height from location to location . Consider July 5 (Figure 13a), where three vertical profiles were taken at Cabras island, St. Croix, and St. Thomas. In this case very similar atmospheric soundings with a moderate trade inversion at ~1800 m and a supra-SAL inversion at 4800 m were observed. For the St. Croix case, the sounding indicates the CBL to be slightly more moist, but this could be due to very localized effects (e.g., flying closer to a cloud). Particle soundings however show more variance. While the Cabras Island and St. Croix vertical profiles are very similar, the profile taken 10 km south of St. Thomas shows about a one-third reduction in particle concentrations uniformly with height. For example, the thin layer between 3800 and 5000 m and the minor maximum at 2800 m are reproduced in al three soundings.

Other gradient days showed more variation in vertical structure of the dust, although for the most part the atmospheric thermodynamic soundings stayed fairly static. Consider the July 10 case (Figure 13b), which showed the strongest gradients of any flight of the study. After the initial vertical profile from Cabras Island, the Navajo proceeded to a point ~50 km north of St. Thomas where mid-visible dust AOTs increased from ~0.15 to 0.2. After completing a descending profile, the Navajo flew south ~120 km to a point west of St. Croix, where AOTs dropped to 0.12. These changes in AOT were coupled with vastly differing dust vertical profiles. At Cabras Island, dust was fairly uniformly distributed from the surface to 2200 m where it monotonically fell off. North of St. Thomas, the dust vertical distribution was more typical for SAL transport with a peak in dust concentration aloft, although there was still some dust enhancement in the MBL and CBL. After flying south to the lowest AOT region, we find the dust has kept its more SAL transport-like nature, with a peak in dust concentrations aloft. However, here we find the SAL dust layer considerably thinner. Accompanying this change is the presence of a very moist layer at 2700-3300 meters, most likely due to cumulus out flow.

The July 22nd case also had its own character. On this flight two soundings were taken at Cabras Island and 120 km south at ~17 degrees N. latitude. Optical depths increased from 0.11 to 0.22 between these two points. Like other days, the trade inversion, CBL and MBL were identical. The

1   most significant difference in the thermodynamic sounding was an increase in the supra-SAL
2   subsidence inversion as we moved south from 3800 to 4200 m and the subsequent deepening of the
3   SAL. On this day while the prominent layer structure remained the same between both locations with
4   uniform increases in amplitude, we find a systematic shift in layer height by about 300 m.
5   Finally, on July 24, we flew the furthest from Puerto Rico than any other part of the study.
6   After completing the Cabras Island sounding, the Navajo flew south to the 16° latitude point(~170 km)
7   where mid-visible optical depths increased from ~0.15 to 0.22. This day demonstrated a tremendous
8   amount of layering over the Cabras Island site with dust dominant in the SAL. Further south, this layer
9   gave way to a more uniform dust distribution, with more elevated dust concentrations below the trade
10   inversions in the CBL
11
12   *3.3.5 Dust Particle Size Issues*
13   Dust particle size distributions are presented in *Savoie et al.* [this issue] and *Reid et al.,* [this
14   issue-a,b] from many aerodynamic, geometric, optical and inversion methods. A "best fit solution" is
15   log-normal with a volume median diameter of 3.5-5 μm and a geometric standard deviation of ~1.9-2.2.
16   However, they show that as dust is a mix of particles with complicated shapes and chemistries, size
17   distributions such as these are difficult to apply. While in this manuscript we are not concerned with
18   the mean dust size distributions, we are interested in how they may be changing with height. Over the
19   course of the PRIDE field study, we did not detect any dramatic shifts in particle size from day to day.
20   This is in part due to the insensitivity of the wing-mounted PMS probes to dust particle sizes.
21   However, as discussed in *Reid et al.,* [this issue-b], by ratioing small and large particle concentrations
22   in the FSSP, some structure can be found.
23   Figure 14 gives particle ratios for 4 selected flights. Here we use the ratio of particles in the
24   1.5-3 μm range from the FSSP as the tracer species as particles in this size range have a mean settling
25   velocity no more than ~25 m per day. These are compared to particles in the 3-6, 6-11, 11-14, and 14-
26   17 μm ranges. All profiles shared some characteristics. The ratio of small to large particles is a
27   minimum in the marine boundary layer. This is probably due to the presence of large sea salt particles.
28   Conversely, the ratio of small to large particles increases significantly in the uppermost 200 m of the
29   dust layer due to gravitational settling.
30   For the most part, the FSSP did not detect any change in particle size ratios within the bulk of
31   the dust layers for SAL conditions. For example, particle ratios did not vary systematically with height
32   for the June 29 and July 20th and 21st cases.. From these figures it also appears that some size
33   separation is visible for very pronounced aerosol layers with the SAL. For example, in the 4150 m
34   layer on July 20th we can track a minimum in the particle ratios as a function of size for 3-6 μm
35   particles, no minimum is detectable. However, for larger particles, it becomes more pronounced ~150
36   m below the dust concentration maximum. Although less pronounced, a minimum is also detectable
37   below the 3600 m dust layer. Similar trends can also be found on the July 21st case. After examining
38   the raw data, we found that these minor changes in the thin layers could not be differentiated from
39   noise. But, over the course of the entire dust layer for the July 20th case (taken between 3000 and 5000
40   m), steeper gradients in particle size ratios are visible.
41   An exception of this behavior was the dust events of July 4th, 5th and 6th where a gradient of
42   ~40% is found between the top and bottom of the dust layer. This can be seen in the July 5 case in
43   Figure 14. All three days of this event exhibited similar behavior. Consider the July 6 case for further
44   examination (Figure 15). Atmospheric thermodynamic soundings along with particle profiles and
45   ratios are shown. On this day a strong SAL was present with a well-defined trade inversion at 1.2 km.
46   Mid-visible optical depths were ~0.25. The vertical profile of estimated mass suggests dust mass is

1   uniformly distributed from the surface to the 3200m level. A second thick layer is also visible from

2   3200 m to 5000m. Based on the 1.5-3 μm particle concentration, a more typical SAL vertical

3   distribution is present. However, larger particles (and hence dust particle mass) is more evenly

4   distributed. Comparing the relative amounts of the two particle size ranges with those in Figures 9-12

5   we can immediately see that smaller particles are strongly enhanced at upper levels. This can be clearly

6   seen in Figure 15 (c) where particle size ratios increase by more than a factor of five with height.

7   It is important to close this section with a reminder that despite these changes in particle size

8   ratios, we did not find a shift in the area and volume distributions from the FSSP. Indeed, all of the

9   cases shown in this section have nearly identical higher moment distributions as the larger particle

10   counts all covary together due to instrument uncertainties. However, we can clearly see that there are

11   differences in the relationship between particle distribution and the relative vertical distribution of the

12   dust. This is discussed in Section 4.

13

14   **3.4 Lidar and Radiosondes.**

15   Navajo data has demonstrated that the vertical distribution of dust mass and size can be at times

16   very complex. Since the Navajo collected data for only 61 hours out of the 28 day field campaign it is

17   difficult to extrapolate these findings to the entire study period and determine the dust's properties to

18   the meteorology of the region. This can be done by examining micropulse lidar (MPL) data from the

19   Cabras Island site along with atmospheric thermodynamic soundings. Figure 16 presents estimated

20   aerosol particle extinction from the MPL from June 28 18Z to July 23 0Z period. Superimposed on

21   these time series are the estimated trade inversion heights (purple dots) derived from radiosondes

22   released at San Juan Airport, PR. *Livingston et al.* [this issue] compared these estimated extinction

23   values to their airborne Sun photometer on the Navajo for four over-flight cases (July 6, 13, 16, and

24   21). Above 1 km in altitude, they found good agreement. The MPL tended to overestimate extinction

25   by ~25% due to the presence of clouds and the use of a uniform lidar ratio for all altitudes.

26   Qualitatively, the comparison between the FSSP and the MPL was excellent (individual comparisons

27   with the FSSP are included in *Livingston et al.* [this issue]).

28   Comparison of Figure 16 with the Navajo data in Figures 9-12 shows that qualitatively the

29   MPL captures the vertical distribution of the dust well. In Figure 15, we can clearly see the passing of

30   the significant dust events: June 28 to ~6:00 Z June 30, 0 Z July 4 to 0 Z July 7, 20 Z to July 8- 0 Z July

31   11, 12 Z July 14 to 20 Z July 16, and 10 Z July 20 to 18 Z on July 22 (No lidar data was available after

32   this time). From the lidar data these events typically lasted 48 hours, although dust was typically

33   present on most days in some amount [*Savoie et al.,* this issue]. Dust maximum altitudes tracked the

34   Navajo data well, with maximum altitudes typically ranging from 3-5 km, with a maximum of 5.5 km

35   on July 21. From the superimposed estimated trade inversion heights from the radiosondes we can see

36   the systematic oscillation of the easterly wave influences with a period of ~2-4 days and maximum

37   inversion heights at 3-5 km. With the advection of a SAL, trade inversions dropped to 1-2 km in

38   altitude.

39   Based on this lidar and radiosonde data, it is clear that the vertical distribution and dynamics of

40   dust is even more complicated than was suggested in the Navajo data. Consider the June 21st event

41   again as what is considered typical "SAL transport." The relatively clean conditions of July 19 gave

42   way to dust and a SAL on the July 20th as the trade inversion descended from 2.5 to 1.5 km. Over the

43   next 48 hours, the trade inversion oscillated between ~1.2 and 2 km. Dust in the SAL was not evenly

44   distributed, but showed consistently like the Navajo data that dust was transported in coherent sheets.

45   These sheets gradually shift in altitude along with the trade inversion, as the SAL is dynamically forced

46   by the large scale supra-SAL subsidence aloft and conditions near the surface. This tracking between

the trade inversion height and dust layers can also be seen in the July 15th case, where despite the presence of dust at lower altitudes a clear SAL dust layer can be seen between 2 and 3 km that is gradually decreasing in altitude along with the trade inversion.

The lidar data also in-part confirms the findings that dust can also be dominant below the trade inversion as well. The June 28-29 case shows clearly and strongly dust in the MBL and CBL despite the presence of a strong SAL. The days following this event showed few particles above 3 km and surface filter measurements by *Savoie et al,* [this issue] found that dust was still the dominant aerosol species in the MBL. The Navajo soundings suggested a gradual shift from more low level transport early in the study, to more uniformly distributed dust, to an upper level SAL transport. Based on the lidar data we find that upper level SAL dust transport occurred sporadically in earlier periods as well. These elevated layers typically passed quickly from four to eight hours. For example, for July 6th after the Navajo flight the lidar shows a dust layer aloft between 2 and 3 km for ~8 hour period even though the SAL extended as low as 1.1 km. Similarly, the July 9th event was initiated with a dust layer aloft between 2 and 4 km.

A valuable aspect of coupling MPL data with the radiosondes is to observe the relationship between dust events and the easterly waves. It is often suggested that dust events follow the passage of easterly waves [e.g., *Carlson and Prospero* 1972; *Westphal et al.,* 1987]. However, after examination of Figure 16 it is unclear if the dust is following, leading or even at times within the easterly wave. With the exception of the very moist cases (e.g., July 14) it often appears that the height of the trade inversion is not an indicator as to the vertical distribution of the dust. In the following section, we analyze MPL, radiosonde, Navajo, and AERONET data and gain insight into the relationship between dust properties and the transport meteorology.

4.0 Analysis of Findings

The PRIDE campaign monitored six significant dust events (five by lidar) each with their own individual character. This data suggests that we may need to reevaluate our conceptual models of long range transport of Saharan dust. Outstanding questions include determining the key factors controlling dust vertical distribution and the relationship between dust and the easterly waves. We can examine these questions by first separating microphysical, local meteorological and long range transport processes. These include dust particle gravitational settling, dry convection and isolated moist convection (i.e., convection not associated with an easterly wave event). Long range transport processes include dust properties at the coast of Africa and interactions with easterly waves and other synoptic scale phenomenon such as large scale differential advection.

Gravitational settling has often been discussed as a first order process for African dust [e.g., *Ellis and Merrill,* 1995]. However, in the context of the PRIDE field campaign gravitational effects likely have little effect on the bulk structure of dust plumes. First, consider that the 98% of the mass and light scattering is associated with particles less than 8 μm in aerodynamic diameter (e.g., see [*Reid et al.,* this issue b]). At 8 μm, settling velocities are 0.25 cm s^{-1}, or 215 m day. Over 6 days of transport, this corresponds to ~1.2 km. A 5 μm aerodynamic diameter particle (where the mass median diameter likely lies), settling would be ~100 m day^{-1}, or 0.6 km over 6 days. Considering the SAL dust layers were typically ~2-3 km thick, gravitational settling could not account for the overwhelming shift of dust from the SAL to the MBL and CBL. Further, as transport times across the Atlantic are roughly the same for the SAL and lower level transport conditions, gravitational settling effects should be equally applied to both cases.

Although gravitational settling does not account for the large scale shifts in dust vertical distribution, it still can give insight into the transport process. Based on calculations above, we would

1   expect to see a great deal of depletion of large particles at the top of SAL layers. But our findings in
2   Figure 14 show depletion only in the uppermost 300 m, not on the order of a km. This would be
3   particularly evident in Figure 14c with the presence of strong shallow layering. Certainly part of this is
4   due to insensitivities of dust size in the FSSP instrument, but we would expect more change than this.
5   Although not in numbers to significantly skew a size distributions, manuscripts such as *Betzer et al.,*
6   [1988] and *Reid et al.,* [this issue-a] have found dust particles larger than 20 μm in Hawaii and Puerto
7   Rico, respectively. A 20 μm particle should settle at velocities greater than 1 cm s^{-1}, or 1 km per day.
8   Recently, *Maring et al.,* [2002] found that after comparing dust aerodynamic particle sizer data in
9   Izaña Tenerefe, Canary Islands with data from the Cabras Island site during PRIDE that there did not
10   appear to be any change in dust particle size distribution for particles less than 7 μm in aerodynamic
11   diameter. Finally, there is also the July 5-6 dust event where we did find a significant gradient in dust
12   size throughout the dust layer. Why is a gradient found on this day but no others? These issues suggest
13   that there are other processes at work which appear to keep dust particles aloft.
14   These gravitational settling issues suggest that perhaps local dry or moist convection may be
15   playing a role. If present, such convection would mix the atmosphere and reduce any particle size
16   gradients. However, convective processes are isolated to specific portions of the atmosphere. By
17   definition, the SAL is neutrally stable without convection. This lack of convective activity is
18   demonstrated by the presence of thin dust layers. In Figure 16 we can see that these layers can exist for
19   12 hours or more. Convection would quickly dissipate any such layering. Hence, it is likely that dry
20   convection is only active in the MBL (i.e., altitudes <500 m) On the other hand, moist convection in
21   the CBL has a more significant role in dust exchange between the SAL and MBL. For the most part,
22   isolated clouds are not mixing dust from deep within the SAL to the surface. While isolated clouds
23   were often observed penetrating the trade inversion by as much as kilometer on days with a strong trade
24   inversion such clouds were rare. Further, such mixing would be evident with increased water vapor
25   mixing ratios inside the SAL. On most days however, moist convection has a strong role to play in the
26   exchange of dust from the trade inversion to the MBL. If dust passes through the trade inversion into
27   the CBL, clouds would mix the dust and transport it into the MBL much more rapidly than gravitational
28   settling. With roughly 20-50% convective cloud cover in the CBL on most days, this process cannot be
29   ignored. On days where there was increased convection with a weak trade inversions (or at high
30   altitudes) such as on July 2-4, 9, and 14, this may be the defining process.
31   We must consider, however, that in the first third of the study period that dust was more
32   uniformly distributed in the atmosphere despite the presence of a strong SAL (e.g., June 28-29, and
33   July 5-6 events). In many case, the concentration of the dust did not vary at all across the trade
34   inversion. On these days, could moist convection be a causal factor? Since there was a strong trade
35   inversion on these days clouds were not penetrating into the SAL. Hence, dust must be transported
36   across the trade inversion by some mechanism before moist convection can act. As discussed above,
37   gravitational settling would allow larger particles to cross the trade inversion. This seems initially
38   plausible as we did in fact see a particle size gradient for the July 5-6 event. With settling velocities on
39   the order of 1.2 and 0.6 km over a 6 day transport period for 8 and 5 μm particles, respectively, such
40   velocities cannot entirely account for such a dramatic shift in vertical distribution. Further, we are still
41   left with the point that why would gravitational settling be important early in the field campaign and not
42   later on?
43   Another possible mechanism is that the trade inversion is evolving along with SAL during
44   transport. *Albrecht et al.* [1979] showed that the height of the trade inversions is dependant on fairly
45   localized effects such as sea surface temperature, surface wind speed, and radiative heating. In
46   addition, the SAL can be squeezed from above by upper level subsidence. We must then recognize that

dust in the SAL and the trade inversion are somewhat de-coupled. Consider the July 21st case where the dust lower boundary is 300 m above the trade inversion. In this case, the trade inversion may have lowered and strengthened over the previous 24 to 48 hours. We can see from Figure 16 that when this occurred, dust layers follow the trade inversion to lower levels. Conversely, for the more uniformly distributed dust cases, the trade inversion may have increased in height with time and/or weakened. This increase in the inversion height would thus entrain dust from above into the CBL and smooth the dust vertical distribution.

This proposed mechanism could probably have a greater impact on dust vertical distribution than gravitational settling alone. But these mechanisms alone cannot explain those circumstances when dust is dominant at lower levels, such as the June 28-29 event. This then leads us to the influence of the easterly waves coupled with differential advection. As discussed in *Carlson and Prospero* [1972] and *Karyampudi et al.* [1999], large dust events seem to follow easterly waves. But, the speed of easterly waves is approximately half that of the mean flow. Hence, some dust laden air should pass through the easterly waves before they reach the western Atlantic Ocean. In the case of PRIDE, where the more moist portions of the easterly waves propagated south of Puerto Rico, it is possible that deep non-precipitating convection will cause the atmosphere and dust to mix. If such mixing were to occur, water vapor would be mixed as well as the dust. Hence, any case where we find a strong SAL with water vapor mixing ratios on the order of 5 g kg^{-1} (e.g., June 28, July 6, 10, 15, 21) excludes the possibility that it passed through an active portion of an easterly wave. However, it is possible for areas below the trade inversion to be transported from the southeast where such mixing could occur in the easterly waves, and then have a dry SAL layer advected into the region aloft from the northeast.

We can test this hypothesis by examining a back trajectory analysis. Figure 17 presents back trajectories for two levels for the June 28, July 5, and July 21st dust cases from the NOAA Realtime Environmental Applications System Hybrid Single-Particle Lagrangian Integrated Trajectory [HYSPLIT, 1997] system. Back trajectories were run for the 300 and 3000 m start altitudes at Puerto Rico for 144 hours. Because these trajectories are made in an area of a data void, they are probably only reliable for 3 days (for example the July 21st case does not even have the trajectories leaving Africa. The July 23rd case, not shown, did not even have mid-level trajectories passing the –50° Longitude line after 6 days). Even so, the trajectories indicate that instead of a northerly component, midlevel air masses in the SAL were more likely to have a more southerly component. These trajectories also show that at times, (such as July 5) differential advection between the levels can be large. Conversely, for the July 21st case, we find both the upper and lower air masses stay together for several days. This was typical for dust events after July 10, 2000. But, even if the upper and lower air masses follow similar tracks, we must consider that they are most likely advected at separate speeds. Hence, lower level dust plumes may arrive at a site ahead or behind a main event. This can be seen in the lidar data for the July 9-10 and July 13 periods and the surface measurements of *Reid et al.,* [this issue-a] and Savoie et al., [this issue]. The maximum dust surface concentrations for the July 9 event were approximately 12 hours behind the maximum in AOT (AOT Max at 15:00Z on July 9, Surface concentration maximum 1:00Z on July 10). A strong surface peak in dust concentration also occurred on July 13, unassociated with any significant AOT event. Hence, although inconclusive, these findings and the back trajectory analysis suggest that at times differential advection is important.

Finally, we must consider the possibility that the vertical distribution of dust is predefined as it passes from Africa to the Atlantic Ocean. It is commonly assumed that dust is transported to sea in elevated SAL layers in the strong easterly trade winds as strong westerly monsoonal flow forms near the coast and blows inland. *Chaipello et al.,* [1995] suggested that in the winter months, when this flow is weak or non-existent, dust can be transported to sea in easterly trade winds at the surface. *Reid et al.,*

1   [2002] argued that based on the soundings at Dakar, monsoonal flow probably did not develop until
2   later than July 5-10. Hence, it is possible that much of the dust for the June 28-29 or even the July 5-6
3   case had in fact left Africa with a similar vertical distributions (i.e., dust in the MBL and CBL). This
4   difference in vertical distribution at the African coast has recently been replicated in the NAAPS and
5   MATCH models [*Colarco et al*, this issue; *Westphal et al.,* this issue].

6

7   **5.0 Implications to Conceptual Models**
8   The findings of the PRIDE project cannot be easily generalized to fit any particular conceptual
9   model. It is likely that to some extent, all of the mechanisms discussed in Section 4.0 play varying
10   roles in determining the dust vertical distribution on an event by event basis. However, we can use
11   this data set to scrutinize preexisting conceptual models and hope to refine them. In particular, the
12   "Upper level SAL transport" (e.g., *Karyampudi et al.,* [1988, 1999] and *Westphal et al.,* [1987]) and the
13   lower level/uniform transport [e.g., *Chaipello et al.,* 1996; *Formenti et al.,* 2001; *Reid et al.,* 2002]
14   warrant further examination.
15   *Karyampudi et al.,* [1988] describes the SAL conceptual model as forming as a result of large dust
16   storms which are mixed up to 5 to 6 km over Africa due to intense solar heating. These dust events are
17   between two consecutive easterly wave troughs. As the dust is advected to the west African coast by
18   easterly trade winds, it is undercut by westerlies in the MBL forming a well-mixed dust layer aloft. As
19   the transport continues westward, the top of the SAL diminishes in altitude slowly due to large scale
20   subsidence aloft. Maximum dust concentrations remain highest in the ridge between the two easterly
21   waves. *Karyampudi et al.,* [1999] (hence referred to as K99) re-examined this model by analyzing a
22   Sept 1994 dust outbreak using Lidar-in Space Technology Experiment (LITE) data coupled with
23   ECMWF meteorology and Meteosat optical depths. Among their conclusions were:

24

25   • There was constantly dust advection off of Africa in association with the Harmattan haze
26   punctuated by fresh high AOT dust outbreaks instead of simply individual dust events..

27

28   • The top of the dust layer over the Atlantic reduced rapidly. They suggest this is due to the fallout of
29   giant particles.

30

31   • High dust concentrations near the southern edge of the SAL can extend downward into the MBL.
32   They suggest this may be a consequence of sedimentation and vertical mixing due to strong vertical
33   wind shears associated with the mid-level jet.

34

35   • The MBL under the SAL appears to be saturated with aerosol particles. They suggest this is due to
36   residual dust particles and sea salt.

37

38   • The trade wind inversion was well defined in the LITE data in the northern edge of the plume.
39   However, the trade inversion was not visible due to dust contamination.

40

41   The findings of the PRIDE campaign support the observational evidence presented by K99, but
42   differs somewhat in interpretation. Let us consider these points individually. First, the findings from
43   the AERONET Sun photometers in Dakar and Cape Verde verify the K99 finding that there is
44   continuous dust advection off of the coast of Africa in September 1994. For the year 2001, this feature
45   also occurred in the summer months (mid-May to mid-October). There is less agreement with their
46   second point that the top of the dust layer is decreasing rapidly due to gravitational settling. Based on

1   our findings, much of the lidar backscatter is due to particles with aerodynamic diameters less than 5
2   μm which do not have an appreciable settling velocity.
3   The final three points listed above from K99 are related to dust vertical distribution. Clearly, the
4   LITE data shows that dust can in fact be significant in the MBL well into the summer transport season.
5   However, K99 interprets this feature as secondary to the principal dust transport. As we have shown
6   dust can in fact have higher concentrations in the MBL than the SAL and cannot easily be dismissed as
7   "residual". Similarly, we have shown that the trade inversion is frequently de-coupled from the SAL.
8   Hence the appearance of a strong gradient in dust in not necessarily indicative of the strength or height
9   of the trade inversion. As K99 pointed out, the lidar data is difficult to interpret due to the presence of
10 hydrated sea salt near the MBL inversion. This can be seen in Livingston et al., [this issue] and our
11 own Figure 16, the increased relative backscattering to extinction ratio due to large sea salt particles can
12 quickly dampen the dust signal. So even here it is not clear if K99 is seeing salt/cloud artifact in the
13 MBL or dust.
14   Finally, K99's finding that dust was found at lower levels in the southern half of the dust plume
15 while more typical "SAL transport" still occurred to the north would indeed suggest vertical mixing and
16 demonstrate the complicated nature of dust transport. Further, such a finding does not necessarily
17 exclude the possibility that the dust left the African coast with that particular north-south gradient in
18 vertical distribution.
19   In contrast to the *Karyampudi et al.,* [1988] conceptual model, *Chaipello et al.,* [1996] suggested a
20 winter time low level dust transport mechanism for those occasions when westerly onshore flow was
21 not present. Consequently, there was no MBL for the SAL to slide over and dust would be transported
22 off of Africa at lower levels. *Reid et al.,* [2002] suggested that this mechanism may extend through the
23 spring. The meteorological data presented by *Chaipello et al.,* [1996], *Reid et al.,* [2002] and this
24 manuscript clearly show that this onshore flow component can weaken thus allowing low level
25 transport. Further, such flow is much more likely to form in the winter months. However, in the
26 context of the PRIDE field campaign conducted in the early summer, what percentage is due to low
27 level transport and what fraction, if any, is due other mixing phenomenon? How does this relate to
28 K99's findings of a north-south gradient in vertical distribution? Additional evidence is found in
29 *Formenti et al.,* [2001], where both low level and more "SAL-ish" transport was observed within just
30 days of one another in South America. This suggests that the both the vertical distribution of dust at
31 Africa and vertical mixing are likely equally important over long periods of time. The PRIDE data
32 shows a gradual change in dust vertical distribution, most likely due to the gradual development of
33 onshore monsoonal flow. However, such flow is unlikely to change over the coarse of 2 to 3 days as
34 would be required to explain *Formenti et al.,* [2001] results.
35   Regardless, of the mechanisms, it is clear that the issues surrounding dust vertical distribution and
36 transport are complicated. Reexamination of other manuscripts yields supporting evidence that lower
37 level transport may be more common than originally thought. As discussed above, K99 and other
38 manuscripts corroborate our findings. While these studies certainly corroborate our findings, like
39 PRIDE they are limited in temporal and spatial scope. Much longer term studies using ground and
40 satellite based remote sensing data are required. Until lidar data is more prevalent more crude methods
41 must be applied to determine the vertical distribution of dust over long periods of time. One
42 opportunity is from co-located Sun photometer and surface filter measurements. *Smirnov et al.,*
43 [2000b] found at Barbados that when averaged over several weeks, surface dust concentrations were
44 highly correlated with dust AOT. However, on a daily basis this correlation reduces significantly
45 indicating that variability in dust vertical distribution is a more common occurrence. A more complete
46 analysis can be found in *Savoie et al.,* [this issue-b].

6.0 Summary and Conclusions

This manuscript gave an overview of the Puerto Rico dust Experiment (PRIDE) field campaign, and in particular focuses on the atmospheric properties of the Caribbean region and dust vertical distribution. This is done by examination of surface based AERONET Sun photometer and micro-pulse lidar data, and airborne data collected on a twin engine Piper Navajo.

At Puerto Rico for PRIDE, six significant dust events reached the island on June 28-29, July 4-6, July 9-10, July 15-16, July 21, and July 23. Mid-visible optical depths at Puerto Rico varied from clean marine conditions at 0.07 to high dust loading periods in excess of 0.5. Average values were ~0.24. In comparison optical depths at the coast of Africa had a higher mean value (~0.45) with peak events up to 1.0. These optical depths are somewhat lower than the previous 3 years, and may be related to a Caribbean wide negative precipitation anomaly.

The vertical distribution of dust in the Caribbean was found to be highly variable during the PRIDE field campaign, with both "typical Saharan Air Layer (SAL)" and lower level transport of dust being observed. Dust frequently reached altitudes of 5 km. The presence of dust in the marine boundary layer was not correlated with any "typical" atmospheric sounding profile, in particular it did not correlate with the strength of the trade inversion in the Caribbean. In fact, as the trade inversion is heavily influenced by local conditions, the SAL and trade inversions can be de-coupled.

The transition between lower level and upper level dust transport occurred slowly over the course of the field study. However, embedded within individual events were well defined layers above the trade inversion. These layers could be persistent for several hundred kilometers in both the along and cross flow directions.

For the most part, we did not find strong gradients in dust particle size with height, except in the uppermost 300 meters of the dust. This including cases with very strong layering. The exception to this behavior was a case occurring during the July 4-6 2000 time frame where strong particle size gradients were observed from the trade inversion up to the maximum dust altitude of 5 km.

We analyze our data and tried to determine the causal factors dictating the vertical distribution of dust. We conclude that the two most likely factors are the dust's vertical distribution as it leaves Africa (i.e., dust is transported across the Atlantic ocean with its vertical character already defined) and the combination of vertical mixing due to moist convection coupled with differential advection. We further analyzed our findings in the context of established conceptual models of dust transport. We scrutinized *Karayampudi et al.,* [1988] and the updated findings of *Karayampudi et al.,* [1999]. During the PRIDE campaign, we found many of the same discrepancies in *Karayampudi et al.,* [1988] as did *Karayampudi et al.,* [1999] using a combination of lidar, satellite, and meteorological data. However, we differ in some of the interpretations of the results.

NWS NCEP Climate Prediction Center, Camp Springs, MD from their web site at
http://www.cpc.ncep.noaa.gov

References

Albrecht, B. A., A model of the thermodynamic structure of the trade-wind boundary layer: Part II Applications, *J. Atmos. Sci., 36*, 90-98, 1979.

Augstein, E., H. Schmidt, and F. Ostapoff, The vertical structure of the atmospheric planetary boundary layer in undisturbed trade winds over the Atlantic Ocean, *Boundary-Layer Meteor., 6*, 129-150, 1974.

Betzer, P. R., K. L. Carder, R. A. Duce, J. T. Merrill, N. W. Tindale, M. Uematsu, D. K Costello, R. W. Young, R. A. Feely, J. A. Breland, R. E. Bernstein, and A. M. Greco, Long-range transport of giant mineral aerosol particles, *Nature*, 336, 569-571, 1988.

Campbell, J.R., D.L. Hlavka, E.J. Welton, C.J. Flynn, D.D. Turner, J.D. Spinhirne, V.S. Scott, and I.H. Hwang, Full-time, Eye-Safe Cloud and Aerosol Lidar Observation at Atmospheric Radiation Measurement Program Sites: Instrument and Data Processing, *J. Atmos. Oceanic Technol.*, accepted, 2001.

Carlson, T. N., and J. M. Prospero, The large-scale movement of Saharan air outbreaks over the northern equatorial Atlantic, *J. Appl. Meteor., 11*, 283-297, 1972.

Carlson, T. N., and R. S. Caverly, Radiative characteristics of Saharan dust at solar wavelengths, *J. Geophys. Res., 82*, 3141-3151, 1977.

Chaipello, I., G. Bergametti, F. Dulac, L. Gomes, B. Chatenet, J. Pimenta, and E. S. Suares, An additional low layer transport of Sahelian and Saharan dust over the north-eastern tropical Atlantic, *Geophys. Res. Lett, 22*, 3191-3174, 1995.

Claquin, T., M. Schulz, Y. Balkanski, and O. Boucher, Uncertainties in assessing radiative forcing by mineral dust, *Tellus, 50B*, 491-505, 1998.

Colarco et al. , *J. Geophys. Res.*, this issue.

Collins, D. R., H. H. Jonsson, J. H. Seinfeld, R. C. Flagan, S. Gasso, D. A. Hegg, P. B. Russell, B. Schmid, J. M. Livingston, E. Ostrom, K. J. Noone, L. M. Russell, and J. P. Putaud, In situ aerosol-size distributions and clear-column radiatve closure during ACE-2, *Tellus, Ser. B., 52*, 498-525, 2000.

Delany, A. C., D. W. Parkin, J. J. Griffin, E. D. Goldberg, and B. E. F. Reinman, Airborne dust collected at Barbados, *Geochim. Cosmochim. Acta*, 31, 885-909, 1967.

Duce, R. A., et al., The atmospheric input of trace species to the world ocean, *Global Biogeochem. Cycle, 5*, 193-260, 1991.

Ellis, W.G., J.T. Merrill, Trajectories for Saharan dust transport to Barbados using Stoke's Law to describe gravitational settling, *J. Appl. Meteor.*, 34, 1716-1726, 1995.

Formenti, P., M. O. Andreae, L. Lange, G. Roberts, J. Cafmeyer, I. Rajta, W, Maenhaut, B. N. Holben, P. Artaxo, and J. Lelieveld, Saharan dust in Brazil and Suriname during the Large-Scale Biosphere-Atmosphere Experiment in Amazonia (LBA)-Cooperative LBA Airborne Regional Exeriment (CLAIRE) in March 1998, *J. Geophys. Res., 106*, 14,919-14,934, 2001.

Fyfe, J. C., Climate simulations of African Easterly Waves. *J. Climate*, **12**, 1747-1769, 1999.

Ganor, E., and Y. Mamane, Transport of Saharan dust across the eastern Mediterranean, *Atmos. Environ.16*, 581-587, 1982.

Gao, Y., Y. J. Kaufman, D. Tanre, D. Kolber, and P. G. Falkowski, Seasonal distributions of aeolian iron fluxes to the global ocean, *Geophys. Res. Lett, 29*, 29-32, 2001.

Giannini, A., Y. Kushnir and M. A. Cane, 2000: Interannual variability of Caribbean rainfall, ENSO, and the Atlantic Ocean. *J. Climate, 13,* 297-311, 2000.

Grist, J. P., Easterly Waves over Africa. Part I: The Seasonal Cycle and contrasts between wet and dry years. *Mon. Wea. Rev. 130*, 197-211, 2002.

Grist, J. P., S. E. Nicholson and A. I. Barcilon, Easterly Waves over Africa. Part II: Observed and modeled contrasts between wet and dry years. *Mon. Wea. Rev. 130,* 212-225, 2002.

Holben, B.N., D.Tanre, A.Smirnov, T.F.Eck, I.Slutsker, N.Abuhassan, W.W.Newcomb, J.Schafer, B.Chatenet, F.Lavenue, Y.J.Kaufman, J.Vande Castle, A.Setzer, B.Markham, D.Clark, R.Frouin, R.Halthore, A.Karnieli, N.T.O'Neill, C.Pietras, R.T.Pinker, K.Voss, and G.Zibordi, An emerging ground-based aerosol climatology: Aerosol Optical Depth from AERONET, *J. Geophys. Res., 106,* 12,067-12,097, 2001.

HYSPLIT4 (HYbrid Single-Particle Lagrangian Integrated Trajectory) Model, Web address: http://www.arl.noaa.gov/ready/hysplit4.html, NOAA Air Resources Laboratory, Silver Spring, MD, 1997.

Janowiak, J. E. and P, Xie, CAMS_OPI: A global Satellite-rain gauge merged product for real-time precipitation monitoring applications. *J. Climate, 12*, 3335-3342, 1999.

Kalnay, E., et al. ,The NCEP/NCAR Reanalysis 40-year Project. *Bull. Amer. Meteor. Soc.*, 77, 437-471, 1996

Karyampudi, V. M., and T. N. Carlson, Analysis and numerical simulations of the Saharan air layer and its effects on easterly wave disturbences, *J. Atmos. Sci., 45*, 3102-3136, 1988.

Karyampudi, V. M., S. P. Palm, J. A. Reagen, H. Fang, W. G. Grant, R. M Hoff, C. Moulin, H. F. Pierce, O. Torres, E. V. Browell, S. H. Melfi, Validation of the Saharan dust plume conceptual model using lidar, Meteosat, and ECMWF data, *Bull. Am. Meteorol. Soc.*, 80, 1045-1075, 1999.

1

2 Maring H., D. L. Savoie, M. A. Izaguirre, L. Custals, and J. S. Reid, Dust aerosol size distribution
3 change during atmospheric transport, *Geophys. Res. Lett.*, submitted, 2002.

4

5 Matsumoto, T., P. B. Russell, C. Mina,, W. Van Ark, and V. Banta, Airborne tracking sunphotometer.
6 *J. Atmos. Ocean. Tech. 4*, 336-339, 1987.

7

8 May, D. A., L. L. Stowe, J. D. Hawkins, and E. P. McClain, A correction for Saharan dust effects on
9 satellite sea surface temperature measurements, *J. Geophys. Res., 94*, 3611-3617, 1992.

10

11 Moulin, C., H. R. Gordon, R. M. Chomko, V. F. Banzon, and R. H. Evans.
12 Atmospheric correction of ocean color imagery through thick layers of Saharan dust, *Geophys. Res.*
13 *Lett.,* 5-8, 2001.

14

15 Myhre, G., and F. Stordal, Global sensitivity experiments of the radiative forcing due to mineral
16 aerosols, *J. Geophys. Res.,106,* 18,193-18, 204, 2001.

17

18 Perry, K. D., T. A. Cahill, R. A. Eldred, D. D. Dutcher, and T. E. Gill, Long-range transport of North
19 African dust to the eastern United States, *J. Geophys. Res.,102*, 11,225-11,238, 1997.

20

21 Pilewskie, P., R. Bergstrom, H. H. Jonsson, J. S. Reid, J. Pommier, J. Livingston, and P.
22 Russell, Solar spectral radiative forcing by dust aerosol during PRIDE, *J. Geophys. Res.*, this issue.

23

24 Prospero, J. M., and T. N. Carlson, Vertical and areal distribution of Saharan dust over the western
25 equatorial North Atlantic Ocean, *J. Geophys. Res., 77*, 5255-5265, 1972.

26

27 Prospero, J. M., R. A. Glaccum, and R. T. Nees, Atmospheric transport of soil dust from Africa to
28 South America, *Nature, 289*, 570-572, 1981.

29

30 Prospero, J. M., Long-term measurements of the transport of African mineral dust to the southeastern
31 United States: implications for regional air quality, *J. Geophys. Res., 104*, 15917-15927, 1999.

32

33 Reid, E. A., J. S. Reid, et al., "Particle Chemistry…, *J. Geophys. Res.*, this issue a.

34

35 Reid, J. S., H. H. Jonsson, H. B. Maring, A. A. Smirnov, D. L. Savoie, S. S. Cliff, M. M. Meier, D. L.
36 Westphal, Comparison of size and morphological measurements of coarse mode dust particles from
37 Africa, *J. Geophys. Res.,* this issue b.

38

39 Reid, J. S., D. L. Westphal, J. Livingston, D. S. Savoie, H. B. Maring, P. Pilewskie, and D. Eleuterio,
40 The vertical distribution of dust transported into the Caribbean during the Puerto Rico Dust
41 Experiment, *Geophys. Res. Lett.*, (in press), 2002.

42

43 Reynolds, R.W., and T. M. Smith, Improved global sea surface temperature analysis using optimum
44 interpolation. *J. Climate, 7*, 929–948, 1994.

45

1   Savoie, D. L., H. B. Maring, and S. A. Christopher, Spectrally-resolved light absorption by Saharan
2   aerosols over the tropical North Atlantic, *J., Geophys. Res.*, this issue-a
3
4   Savoie, D. L., A. Smirnov, J. Reid, H. B. Maring, and B. N. Holben, Vertical distribution of Saharan
5   dust aerosols over the tropical North Atlantic based on ground-based dust measurements and
6   AERONET aerosol optical depths, *J., Geophys. Res.*, this issue-b
7
8   Smirnov A., B. N. Holben, T. F. Eck, O. Dubovik and I. Slutsker, Cloud screening and quality control
9   algorithms for the AERONET data base. *Remote Sens. Environ.*,73, 337-349, 2000a.
10
11   Smirnov, A., B.N.Holben, D.Savoie, J.M.Prospero, Y.J.Kaufman, D.Tanre, T.F.Eck, and I.Slutsker,
12   Relationship between column aerosol optical thickness and in situ ground based dust concentrations
13   over Barbados, *Geoph. Res. Lett., 27*, 1643-1646, 2000b.
14
15   Smirnov, A., B.N.Holben, Y.J.Kaufman, O.Dubovik, T.F.Eck, I.Slutsker, C.Pietras, and R.Halthore,
16   Optical properties of atmospheric aerosol in maritime environments, *J.Atm.Sci., 59*, 501-523, 2002.
17
18   Sokolik, I. N., D. M. Winker, G. Bergametti, D. A. Gillette, G. Carmichael, Y. J. Kaufman, L. Gomes,
19   L. Schuetz, and J. E. Penner, Introduction to special section: Outstanding problems in quantifying the
20   radiative impacts of mineral dust, *J. Geophys. Res., 106*, 18,015-18,028, 2001.
21
22   Spinhirne, J. D., Rall, J., and V. S. Scott, Compact eye-safe lidar systems. *Rev. Laser Eng.*, 23, 26-32,
23   1995.
24
25   Swap R., M. Garstang, S. Greco, R. Talbot, and P. Kallberg, Saharan dust in the Amazon Basin, *Tellus,*
26   *144B*,133-149,1992.
27
28   Swap, R, M. Garstang, S. A. Macko, P. D. Tyson, W. Maenhaut, P. Artaxo, P. Kallberg, and R. Talbot,
29   The long-range transport of southern African aerosols to the tropical South Atlantic, *J. Geophys. Res.,*
30   *101*, 23,777-23,791, 1996a.
31
32   Swap, R., S. Ulanski, M. Cobbett, and M. Garstang, Temporal and spatial characteristics of Saharan
33   dust outbreaks,*J. Geophys. Res.,* 101, 4205-4220, 1996b.
34
35   Talbot, R.W., M. O. Andreae, H. Berresheim, P. Artaxo, M. Garstang, R. C. Harriss, K. M. Beecher,
36   and S. M. Li, Aerosol chemistry during the wet season in central Amazonia: the influence of long-range
37   transport, *J. Geophys. Res., 95*, 16,955-16,969, 1990.
38
39   Tanre, D., Y. J. Kaufman, B. N. Holben, B. Chatenet, A. Karnieli, F. Lavenu, L. Blarel, O. Dubovik, L.
40   A. Remer, and A. Smirnov, Climatology of dust aerosol size distribution and optical properties derived
41   from remotely sensed data in the solar spectrum, *J. Geophys. Res., 106*, 18,205-18,219, 2001.
42
43   Tegen, I. and I. Fung, The influence on climate forcing of mineral aerosols from disturbed soils,
44   *Nature, 380*, 419-422, 1996.
45

1 Welton, E.J., J.R. Campbell, T.A. Berkoff, J.D. Spinhirne, S. Tsay, and B. Holben, First Annual
2 Report: The Micro-pulse Lidar Worldwide Observational Network, Project Report, 2001a.
3
4 Welton, E.J., K.J. Voss, P.K. Quinn, P.J. Flatau, K. Markowicz, J.R. Campbell, J.D. Spinhirne, H.R.
5 Gordon, and J.E. Johnson, Measurements of aerosol vertical profiles and optical properties during
6 INDOEX 1999 using micro-pulse lidars, *J. Geophys. Res.*, in press, 2001b.
7
8 Welton, E.J., and J.R. Campbell, Micro-pulse lidar signals: Uncertainty analysis, *J. Atmos. Oceanic*
9 *Technol.*, submitted, 2001.
10
11 Westphal, D. L., O. B. Toon, and T. N. Carlson: A two-dimensional numerical investigation of the
12 dynamics and microphysics of Saharan dust storms. *J. Geophys. Res.*, 92, 3027-3049, 1987.
13
14
15
16
17
18
19
20 **Figure Captions:**
21
22 Figure 1. (a) Monthly averaged AVHRR Pathfinder aerosol optical thickness of the North Sub-tropical
23 Atlantic Basin for the month of July 2000. (b) GOES 8 visible image for the Caribbean region at 15:30
24 UTC on July 5th, 2000.
25
26 Figure 2. Picture of SSC San Diego Navajo taken during PRIDE and annotated with instrument
27 placements (Photo by Hal Maring, University of Miami).
28
29 Figure 3. NCAR/NCEP reanalysis of 600 mb July 2000 mean wind vector field and zonal wind
30 anomaly.
31
32 Figure 4. NCEP precipitation statistics for Tambacouda, Senegal and Ouagadou, Burkina Faso
33
34 Figure 5. Example thermodynamic soundings from radiosondes released at San Juan Airport, PR, for
35 (a) July 21 2000 the classic Saran Air Layer and (b) July 7 2000 when the region was under the
36 influence of easterly waves.
37
38 Figure 6. Year 2000 AERONET daily average aerosol optical thickness (AOT) at a wavelength of 670
39 nm measurements taken at (a) Cape Verede, (b) Dakar, (c) Barbados, and (d) Puerto Rico. The Puerto
40 Rico data was taken from the Roosevelt Roads site during the PRIDE study period (until 24 July) and
41 from the La Paguera site for the remaineder of the year.
42
43 Figure 7. AERONET daily average aerosol optical thickness (AOT) at a wavelength of 670 nm
44 measurements for the PRIDE study period. (a) Cape Verede, (b) Dakar, (c) Barbados, and (d) Puerto
45 Rico.
46

1 Figure 8. Aerosol optical thickness (AOT) as a function of wavelength for various days at (a) Cape
2 Verde and (b) Roosevelt Roads, PR.
3
4
5 Figure 9. Atmospheric soundings from the Navajo aircraft for four days with clean marine conditions
6 (July 8, 11, 17, 19, 2000). First column, thermodynamic state variables temperature (T-thick solid),
7 dew point (T_d-thin solid), equivalent potential temperature (θ_e), and water vapor mixing ratio (ω_v-tight
8 dash). Second column, FSSP number concentration (1.5-3 μm-thick solid, 3-17 μm-thin solid), and
9 estimated coarse mode particle concentration (dashed). Column 3, estimated fine mode mass
10 concentration from the PCASP for particles <0.3 μm (solid) and 0.3-1.1 μm (dashed).
11
12 Figure 10. Same as Figure 9 but for four days with SAL transport conditions (July 20-23, 2000). Note
13 the scale change for column 3.
14
15 Figure 11. Same as Figure 9 but for four days the first week of the study when dust was dominant
16 below the trade inversion (June 28, and July 3, 4, and 5).
17
18 Figure 12. Same as Figure 9 but for the middle of the study when dust was in transition between lower
19 level and SAL transport (July 10, 13, 15, 16).
20
21 Figure 13. Atmospheric soundings from the Navajo aircraft for four days when a gradient was seen in
22 dust concentrations and vertical profiles. (July 5, 10, 22, and 24, 2000). First column, temperature and,
23 dew point). Second column, FSSP number concentration (1.5-3 μm-thick solid, 3-17 μm-thin solid),
24 and estimated coarse mode particle concentration (dashed). Column 3, GOES-8 image taken at flight
25 time with flight track overlaid.
26
27 Figure 14. Dust vertical distribution of dust particle size ratios for June 28, July 5, 20, and 21, 2000.
28 First column, FSSP number concentration in the 1.5-3 μm diameter range. Second column ratios of the
29 number of particles in the 3-6, 6-11, 11-14, and 14-17 μm diameter size range to the number
30 concentration in the 1.5-3 μm diameter range.
31
32 Figure 15. Vertical distribution information for July 6, 2000. (a) thermodynamic state variables
33 temperature (T-thick solid), dew point (T_d-thin solid), equivalent potential temperature (θ_e), and water
34 vapor mixing ratio (ω_v-tight dash). (b), FSSP number concentration (1.5-3 μm-thick solid, 3-17 μm-
35 thin solid), and estimated coarse mode particle concentration (dashed). (c) ratios of the number of
36 particles in the 3-6, 6-11, 11-14, and 14-17 μm diameter size range to the number concentration in the
37 1.5-3 μm diameter range.
38
39 Figure 16. Estimated atmospheric light extinction values from the micropulse lidar station at Cabras
40 Island. Purple dots indicate the estimated trade inversion height from the San Juan Airport radiosonde
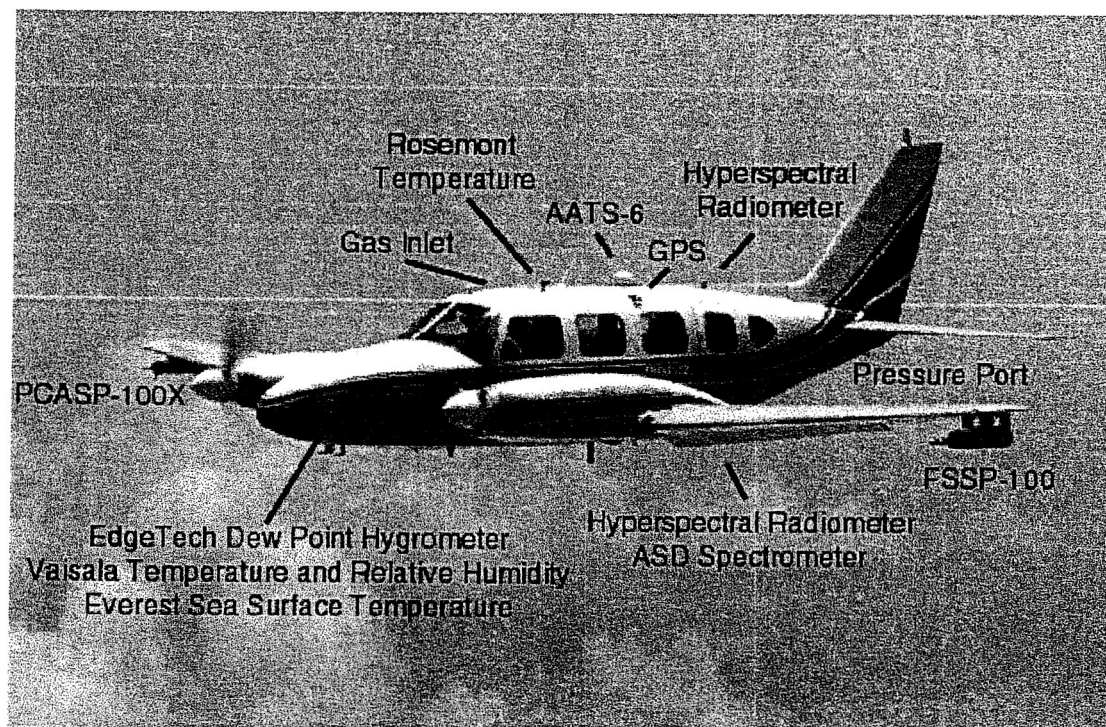41 data.
42
43 Figure 17. 300 and 3000 m READY/HYSPLIT 144 hour back trajectories from Roosevelt Roads,
44 Puerto Rico. (a) June 28, 14:00Z start time, (b) July 5, 14:00Z start time, (c) July 21, 14:00Z start time.

Table 1. Summary flight information for the SSC-SD Navajo Profile aerosol optical depth (AOT) is the difference between the AOT at the surface and the AOT at the Saharan Air layer (SAL) top. EH Inversion is the height of the extratropical high forming a dry Supra-SAL layer. Estimated dust loading was approximated by subtracting the clean marine background AOT (0.07) from the profile AOT and then dividing by the average mass extinction efficiency of dust for PRIDE ($\sim$0.75 m^2 g^{-1} [*Savoie et al.*, this issue]).

Date	Data Collection Period (UTC)	Number of Vertical Profiles	MBL Height (m)	Trade Inversion (m)	EH Inversion	Cabras Island Profile AOT	Estimated Dust Loading (g m^{-2})
6/28	13:15-15:00	2	450	1100	4100	0.48	0.55
6/30	13:00-16:30	4	550	1600	3700	0.24	0.23
7/1	13:00-16:15	3	750	2000	2500	0.13	0.08
7/3	14:30-17:00	2	450	1800	4100	$\sim$0.20	0.17
7/4	14:00-17:15	4	300	2000	4800	0.29	0.29
7/5	13:15-16:00	3	450	1900	4800	0.35	0.37
7/6	13:00-16:30	4	400	1000	4500	0.25	0.24
7/8	13:00-15:15	2	700	none	none	$\sim$0.06	<0.03
7/10	13:15-16:30	3	650	1600	3300	0.15	0.11
7/11	13:00-16:15	3	450	2800	3100	0.06	<0.03
7/12	13:00-16:15	3	800	2100	4000	0.12	0.07
7/13	13:30-17:00	2	500	1350	3000	0.17	0.13
7/15	14:15-18:00	3	500	1150	4800	0.26	0.25
7/16	13:15-16:15	3	800	1950	4000	0.23	0.21
7/17	13:00-14:30	2	500	2000	3000	0.07	<0.03
7/19	14:15-15:30	2	400	2100	3100	0.06	<0.03
7/20	14:15-17:00	3	500	2300	5500	0.27	0.27
7/21	13:15-16:15	3	600	1350	4950	0.35	0.37
7/22	13:30-16:00	2	500	1950	3800	0.11	0.05
7/23	12:30-16:00	3	200	1650	4200	0.30	0.31
7/24	13:15-16:15	2	450	2000	3900	0.15	0.11
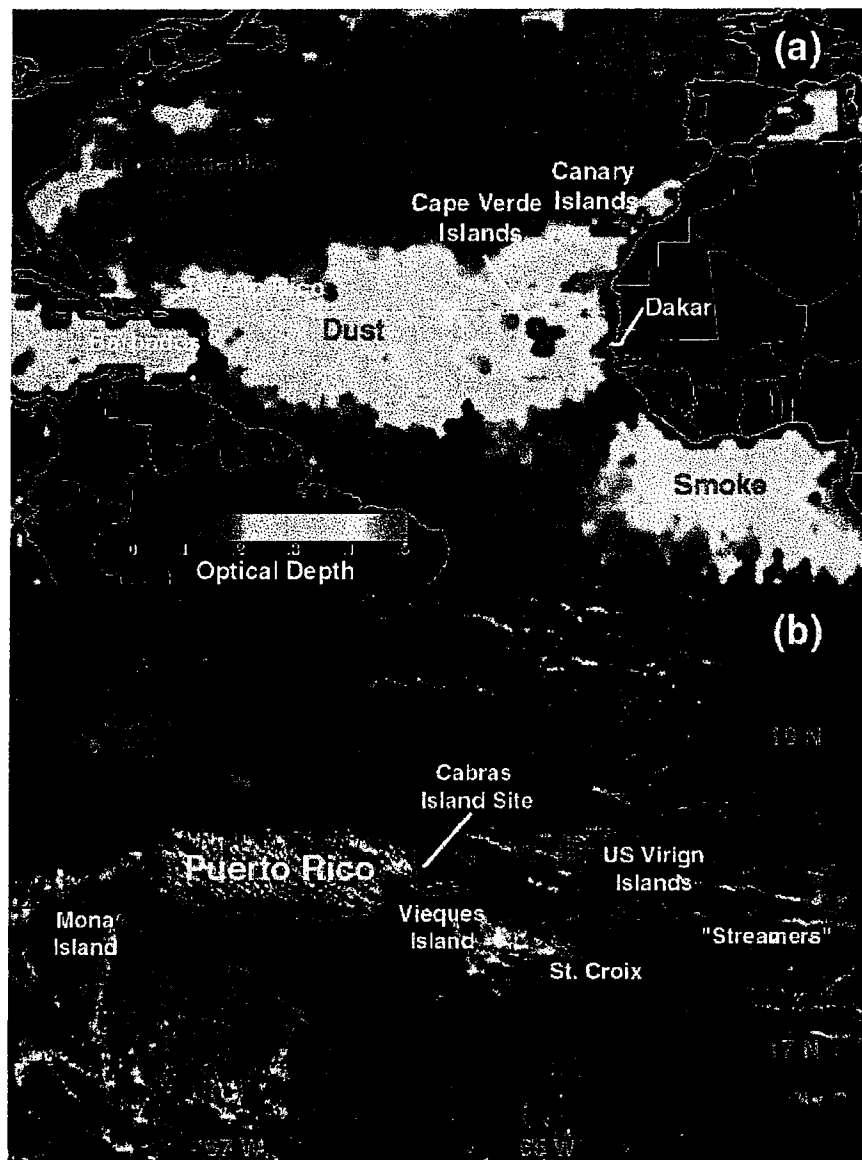
Reid et al., Figure 1.

Reid et al., Figure 2

600mb Vector Wind (m/s) Composite Mean
Jul 2000
NCEP/NCAR Reanalysis

600mb Zonal Wind (m/s) Composite Anomaly
Jul 2000
NCEP/NCAR Reanalysis
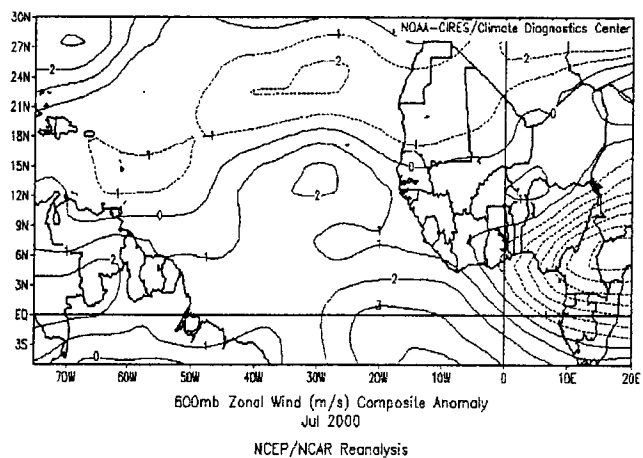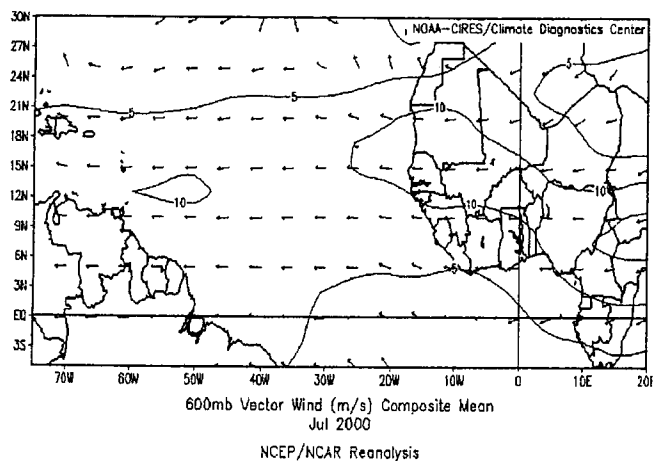
Reid et al., Figure 3

Reid et al., Figure 4

(a)

Extra-SAL Layers
SAL Top
Saharan
Air Layer
Trade Inversion
Convective Boundary Layer
Marine Boundary Layer Inversion
Marine Boundary Layer

— Temperature
- - Dew Point
— Mixing Ratio
-·-· Relative Humidity

Temperature ($^{\circ}$C), Mixing Ratio (g kg^{-1}), and Relative Humidity (%)

(b)

Subtropical High
Layer Aloft
Weak Trade Inversion
Convective Boundary Layers
Marine Boundary Layer Inversion
Marine Boundary Layer

— Temperature
- - Dew Point
— Mixing Ratio
-·-· Relative Humidity

Temperature ($^{\circ}$C), Mixing Ratio (g kg^{-1}), and Relative Humidity (%)

Reid et al., Figure 5

Reid et al., Figure 6
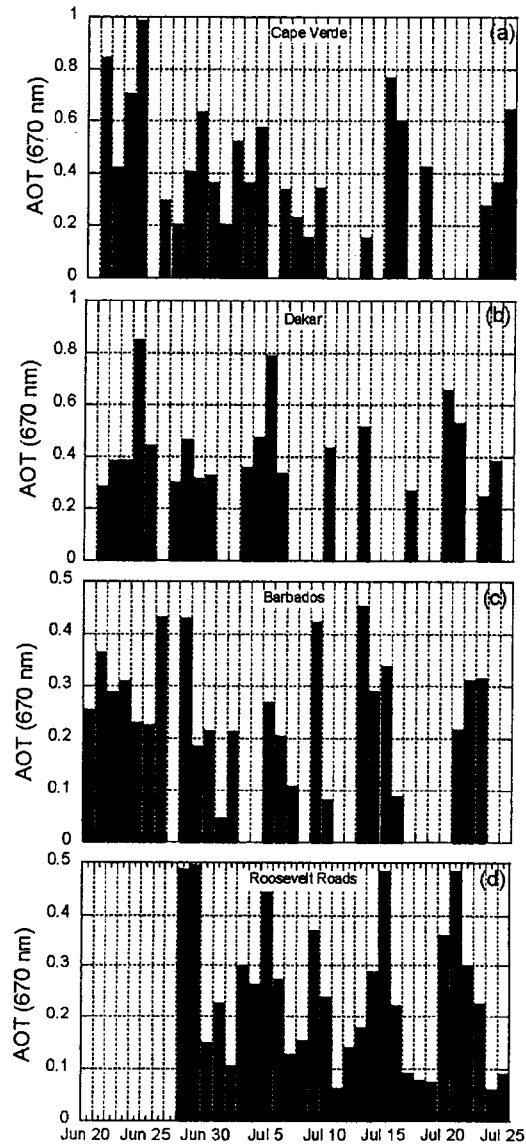
Reid et al., Figure 7
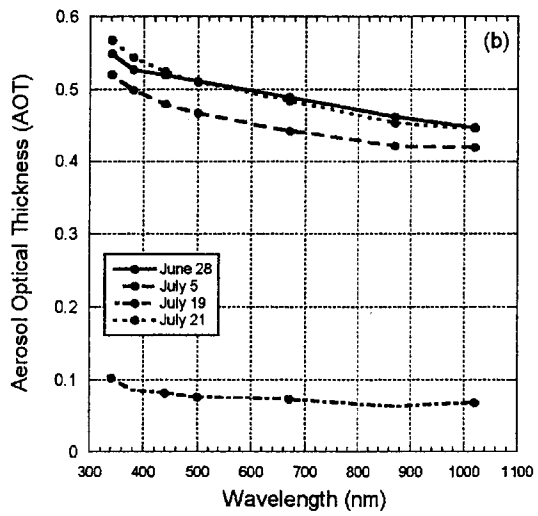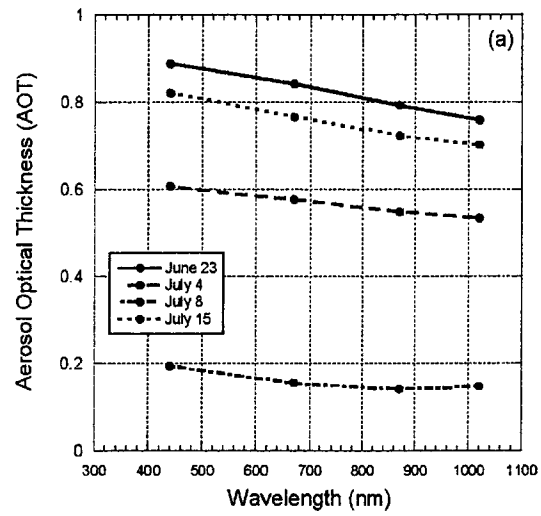
Reid et al., Figure 8
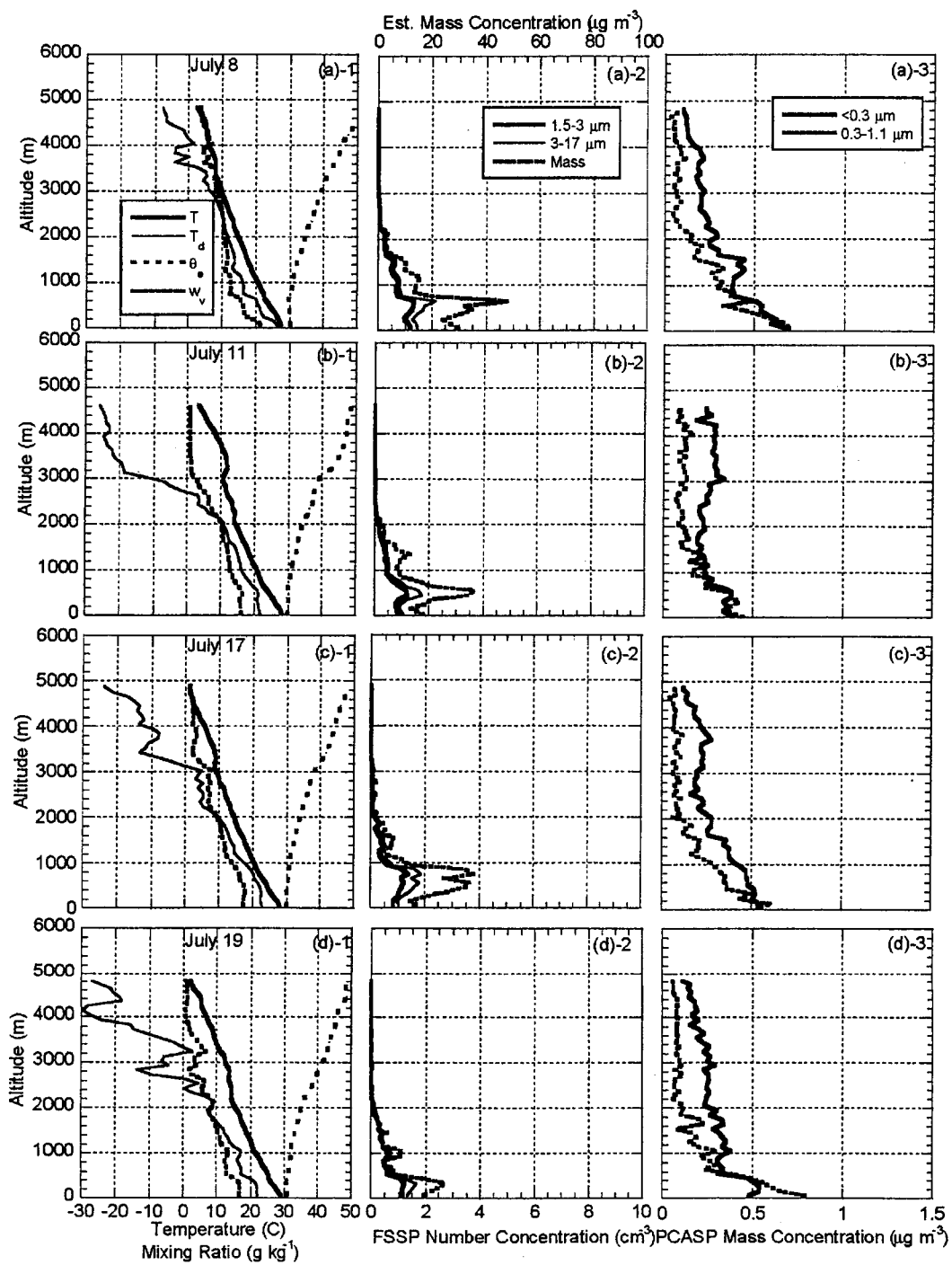
Reid et al., Figure 9
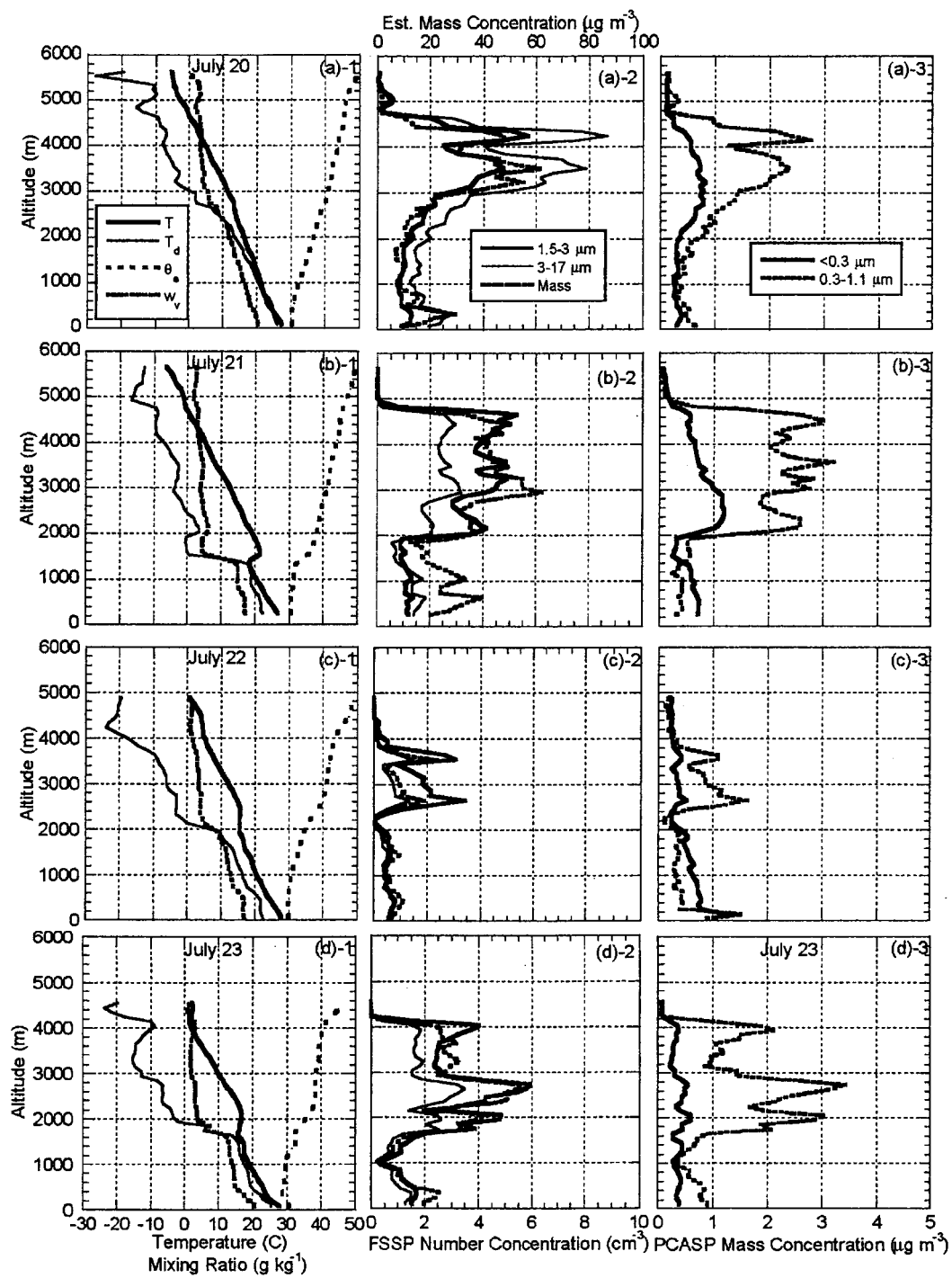
Reid et al., Figure 10
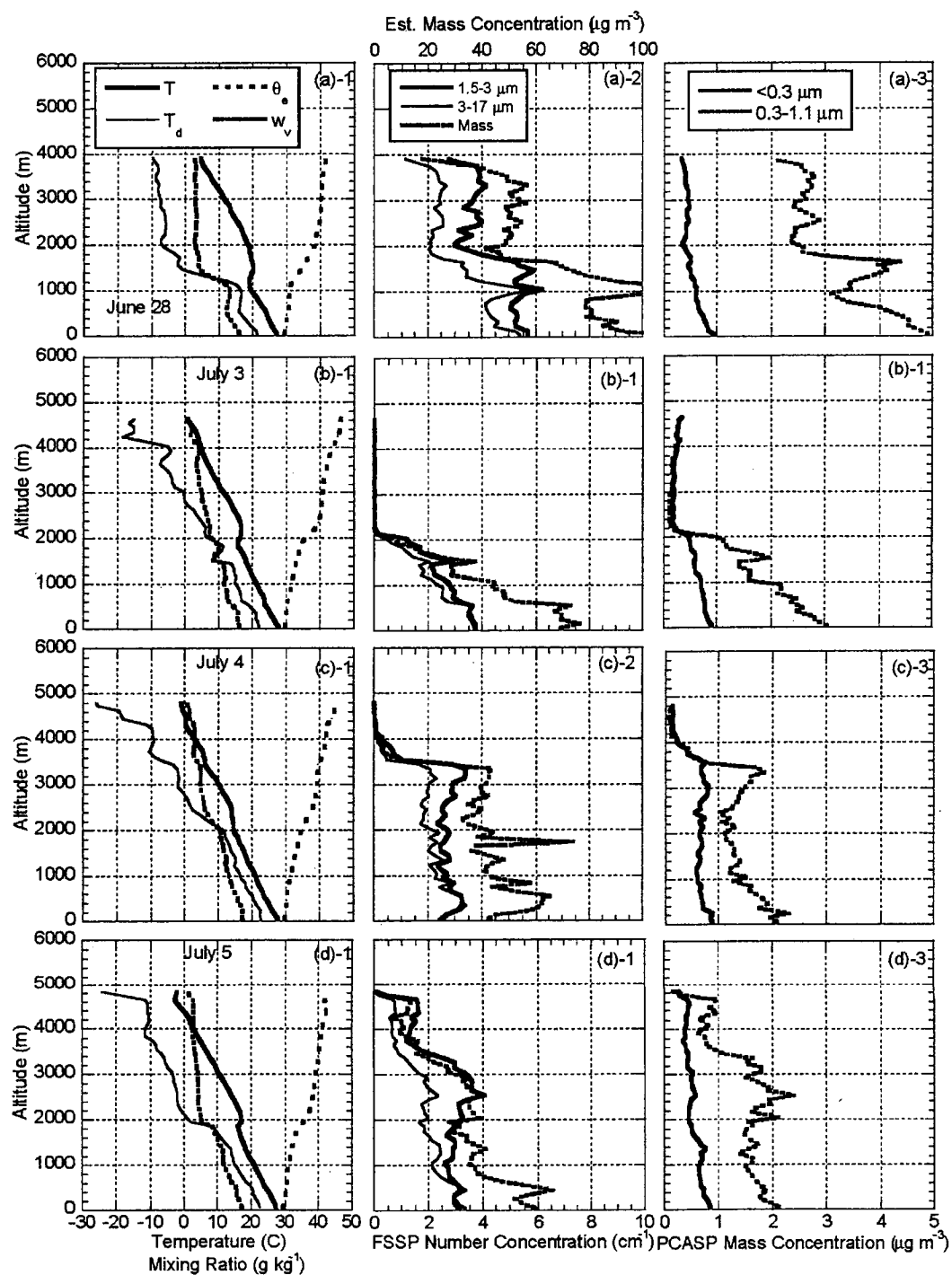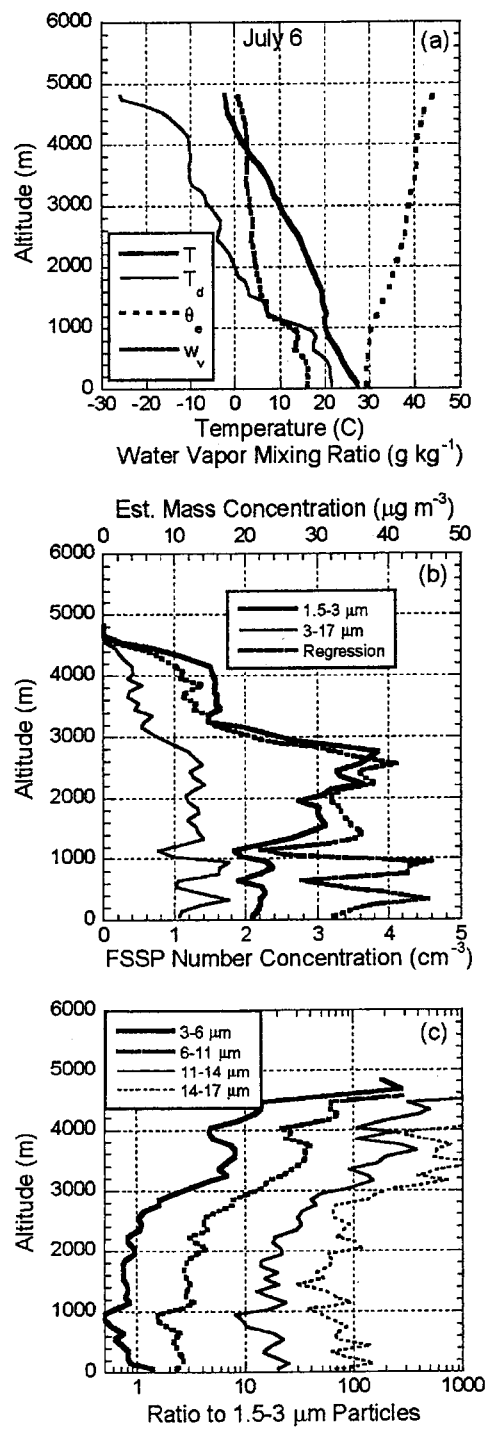
Reid et al., Figure 11
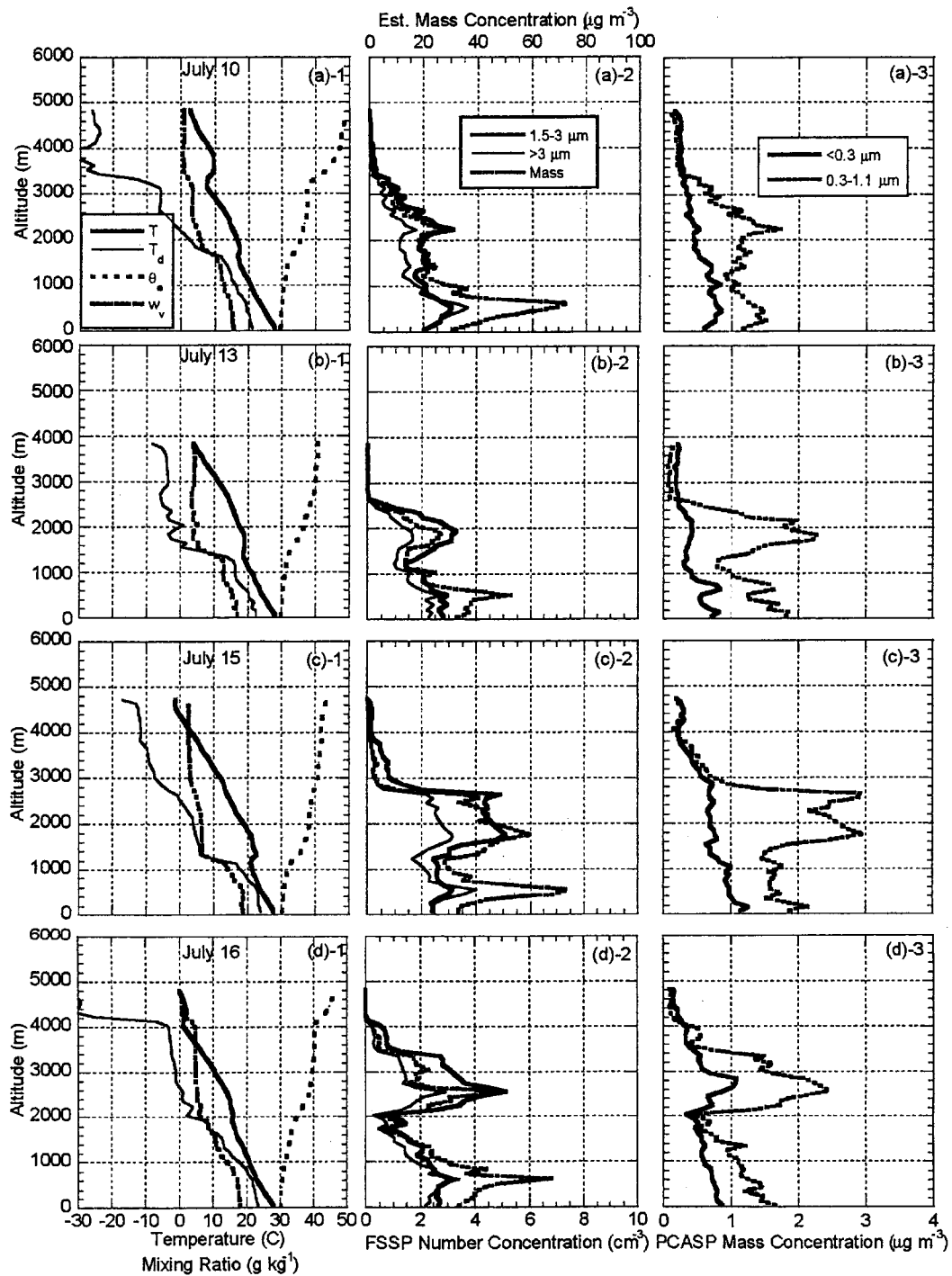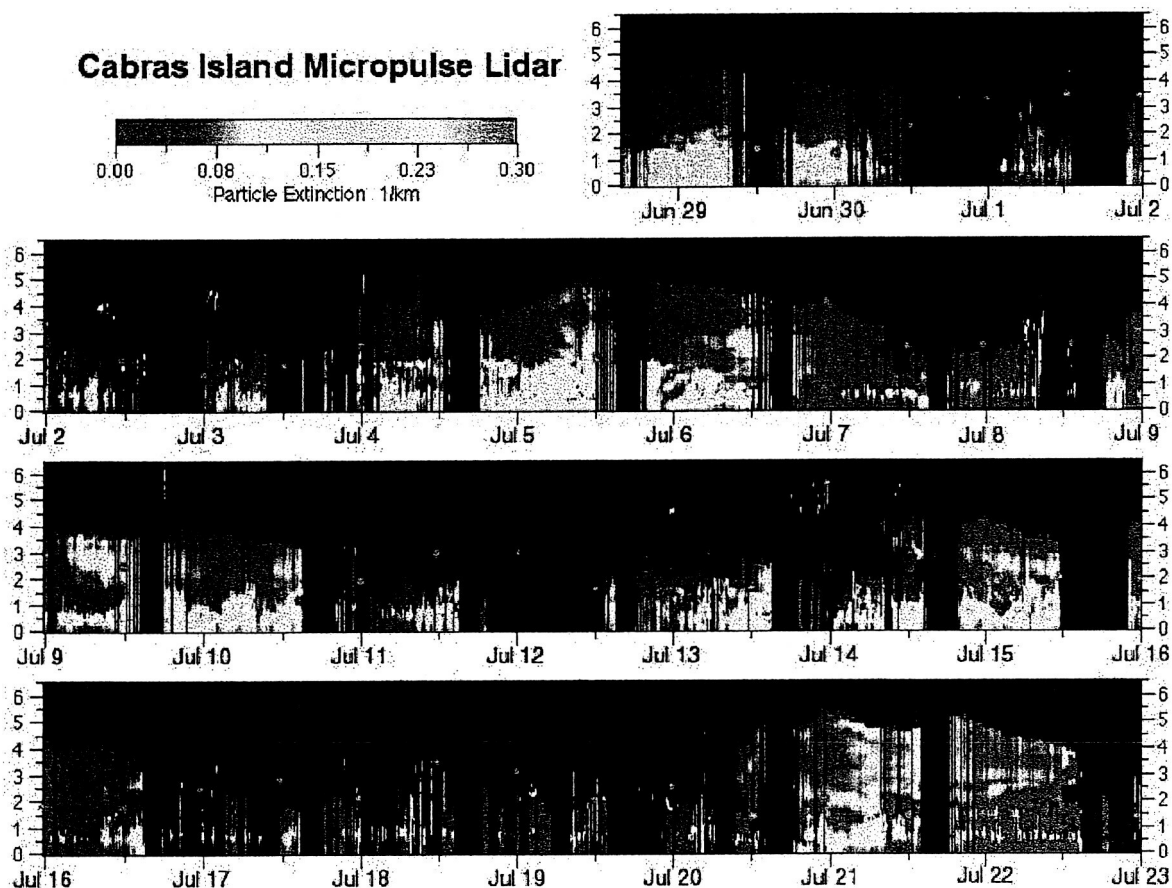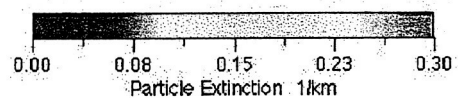
Reid et al. Figure 12
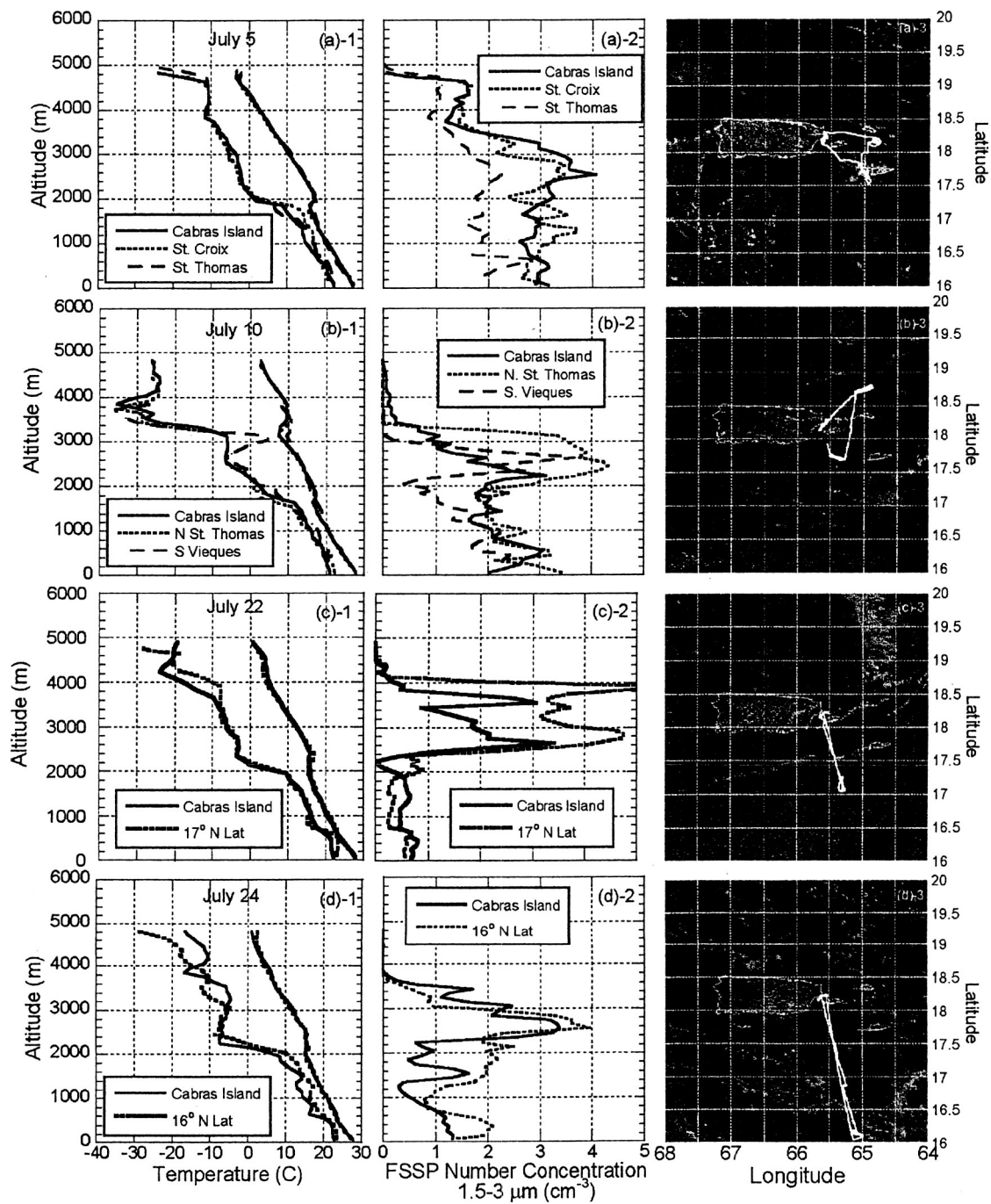
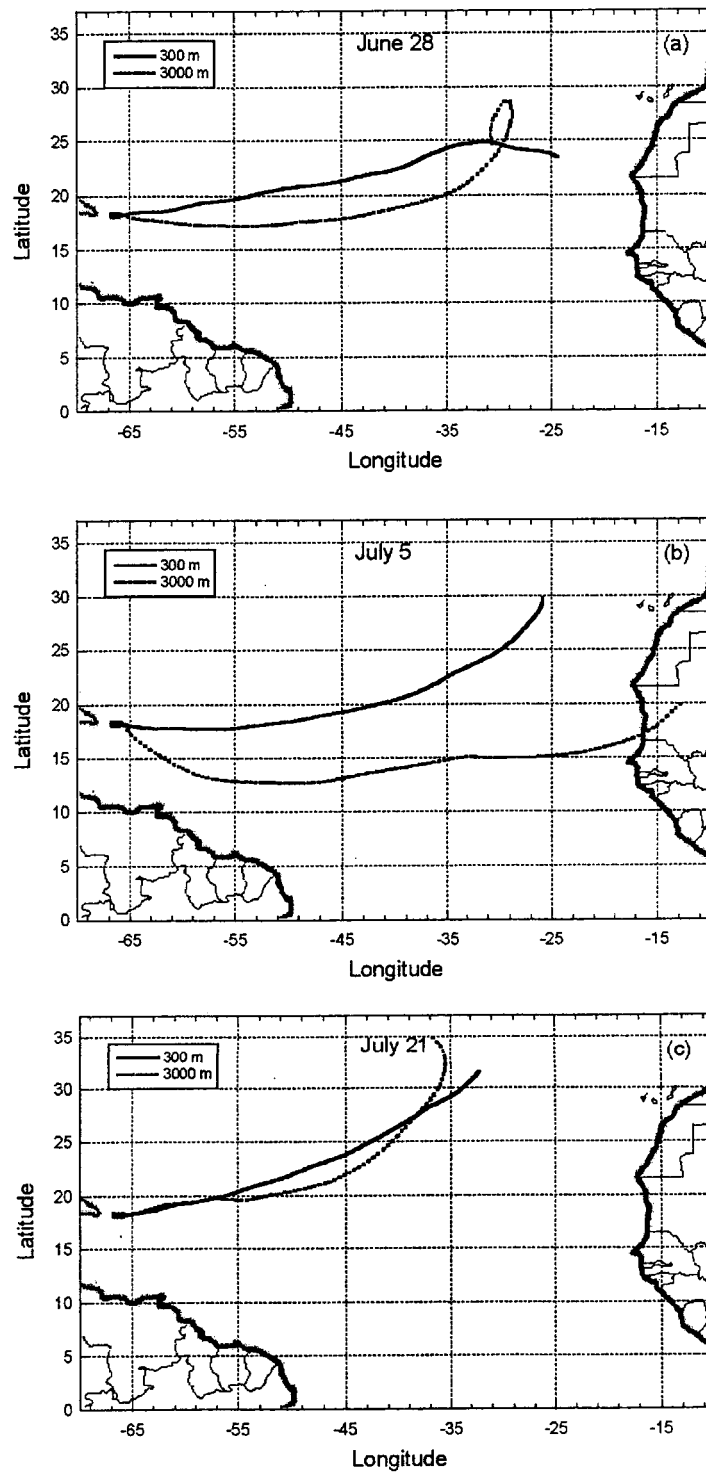Reid et al., Figure 13
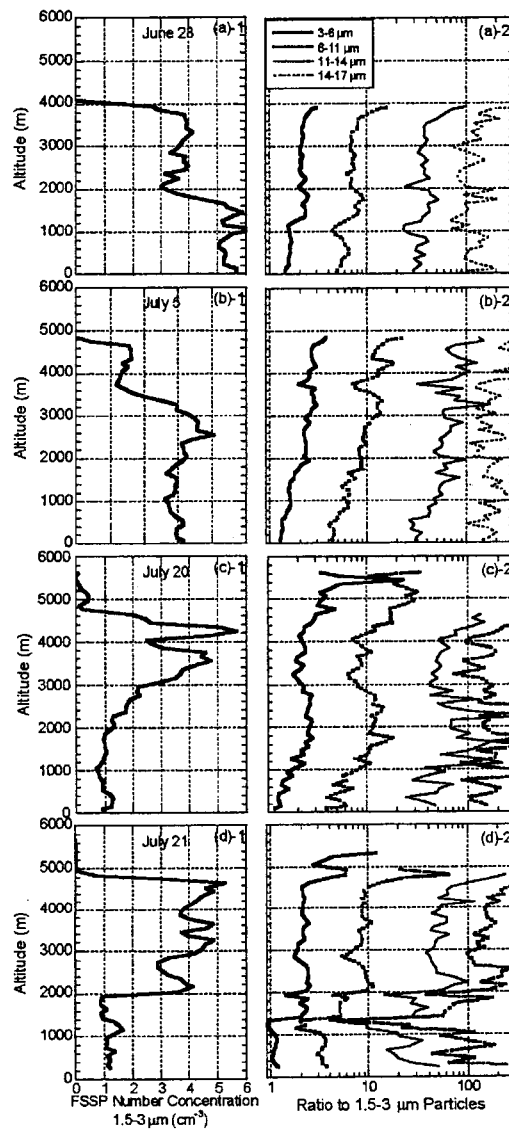
Reid et al., Figure 14

Reid et al., Figure 15

Cabras Island Micropulse Lidar

Reid Figure 16

Reid et al., Figure 17